Propulsion and Energy Forum
July 28-30, 2014, Cleveland, OH
50th AIAA/ASME/SAE/ASEE Joint Propulsion Conference

Effects of Injector Design on Combustion Stability in Hybrid Rockets Using Self-Pressurizing Oxidizers

Benjamin S. Waxman*, Jonah E. Zimmerman†, Brian J. Cantwell‡
Stanford University, Stanford, CA 94305

and

Gregory G. Zilliac§
NASA Ames Research Center, Moffet Field, CA 94035

Interest in nitrous oxide based hybrid rockets is at an all time high. Nitrous oxide (N_2O) is a unique oxidizer because it exhibits a high vapor pressure at room temperature ($\approx$ 730 psia or 5.03 MPa). Due to this high vapor pressure, liquid nitrous oxide can be expelled from a tank without the use of complicated pumps or pressurization systems required by most traditional liquid rocket systems. This results in weight savings and design simplicity. Additional benefits of nitrous oxide include storability, ease of handling, and relative safety compared to traditional liquid oxidizers. The design and modeling of injectors for use with high vapor pressure propellants such as nitrous oxide is made complicated due to the possibility of two-phase flow. The operating pressures within rocket propellant feed systems can often drop below the vapor pressure for these unique propellants, especially within the injector. Injectors operating under these conditions are likely to exhibit cavitation, resulting in significant vapor formation and limitation of mass flow rate. With the introduction of two-phase flow, a critical flow regime can be observed, where the flow rate is independent of backpressure (similar to choking). For a simple orifice style injector, it has been demonstrated that critical flow occurs when the downstream pressure falls sufficiently below the vapor pressure, ensuring bulk vapor formation within the injector element. It has been proposed to leverage the insensitivity of critical mass flow rate to downstream pressure as a means of preventing the occurrence of feed system coupled combustion instabilities in hybrid rockets utilizing nitrous oxide. The Peregrine Sounding Rocket is a hybrid rocket that runs on paraffin wax and nitrous oxide. Its development is a joint effort between NASA Ames Research Center, Stanford University, and Space Propulsion Group, Inc. For years, progress of the Peregrine program has been hampered by combustion instability problems. Based upon results from the aforementioned small scale injector experiments, a powerful, yet simple solution to the so-called feed system coupled combustion instability was discovered, the details of which are presented. This work also led to the invention of a new class of rocket propellant injectors designed specifically to decrease the likelihood of this type of combustion instability. An in-depth discussion of the proposed design and operation of this novel injection scheme is included, along with the presentation of some prototype cold flow testing results which served as a successful proof of concept.

Nomenclature

a	=	effective average sound speed
A	=	cross-sectional area
C_d	=	discharge coefficient
D	=	injector hole diameter
f	=	natural mode frequency
g_o	=	standard acceleration due to gravity
l	=	wavelength of the natural acoustic mode
L	=	injector hole length
$\dot{m}$	=	mass flow rate
M	=	molecular weight
P	=	pressure
T	=	temperature
u	=	fluid velocity
Z	=	compressibility factor

Subscripts

1	=	location upstream of injector
2	=	location at exit or downstream of injector
c	=	thermodynamic critical conditions
$diff$	=	diffuser

*Ph.D. Recipient, SPaSE Lab , Department of Aeronautics & Astronautics, Stanford University, CA, AIAA Student Member.
†Ph.D. Candidate SPaSE Lab , Department of Aeronautics & Astronautics, Stanford University, CA, AIAA Student Member.
‡Edward C. Wells Professor, Department of Aeronautics & Astronautics, Stanford University, CA, AIAA Fellow.
§Research Scientist, NASA Ames Research Center/M.S. 260-1, Moffett Field, CA, AIAA Member.

inj	=	injector
ox	=	oxidizer
s	=	saturation
$super$	=	supercharge
t	=	throat
$trip$	=	thermodynamic triple point
v	=	vapor

Symbols

α	=	cavitating venturi injector coefficient
Δ	=	difference across injector
ω	=	acentric factor
ρ	=	density

I. Introduction

Hybrid rocket propulsion has seen considerable renewed interest over the past decade. Universities, private companies, and governmental organizations around the globe are currently developing a wide range of hybrid rocket technologies. Self-pressurizing rocket propellants have recently seen increased interest, especially in the field of hybrid rocket propulsion. Specifically, nitrous oxide (N_2O) has recently seen a surge in popularity as a self-pressurizing liquid oxidizer for use in hybrid rockets, ranging from small scale amateur and academic projects to multiple full-scale development programs [1,2]. Nitrous oxide has a vapor pressure, P_v (also called saturation pressure, P_s) of approximately 730 psi (5.03 MPa) at room temperature. This makes nitrous oxide an attractive propellant choice for hybrid rockets because it can be expelled from a storage tank without the need for complicated pressurization systems or turbopumps (hence the term self-pressurizing). Nitrous oxide is highly storable, relatively nontoxic, and easy to handle. Therefore, it is generally considered a safer alternative to the more traditional oxidizers typically used in launch systems today (such as LOX, N_2O_4, etc.). Some important thermodynamic properties of nitrous oxide are outlined in Table 1 and Fig. 1.

Table 1. Important thermodynamic properties of N_2O. This data was calculated using REFPROP [3,4].

Property	Units	N_2O
M	amu	44.013
P_c	psia (MPa)	1050.8 (7.25)
P_{trip}	psia (MPa)	12.7 (0.09)
T_c	^oC (K)	36.5 (309.7)
T_{trip}	^oC (K)	-90.2 (183.0)
ρ_c	$\frac{kg}{m^3}$	452.0
Z_c		0.273
ω		0.160

The purpose of the hybrid rocket injector is to provide the desired mass flow rate of oxidizer to the combustion chamber, while sufficiently atomizing the liquid to allow for rapid vaporization of droplets. An oxidizer injector generally consists of one or more holes, orifices, or passageways (potentially hundreds) which restrict the total cross-sectional flow area, thus restricting, or metering the mass flow rate. When used in the self-pressurizing fashion, nitrous oxide is stored at or around its vapor pressure. Therefore the operating pressures within the feed system, especially within the injector, can reach values below the vapor pressure of the liquid, resulting in possible vaporization of the oxidizer and the introduction of two-phase flow. This type of vaporization (by pressure drop) is termed cavitation, as opposed to the more common term, boiling, which refers to vaporization due to heat addition. Cavitation can result in the limitation of mass flow rate through the injector, as demonstrated in Fig. 2 which shows the variations that result in the measured injector discharge coefficient C_d over a series of cold flow and hot fire tests during the Peregrine Hybrid Sounding Rocket Program (details of which will be discussed in Section II). It is clear from Fig. 2 that the discharge coefficient can vary greatly, depending on the operating conditions of the injector (injector pressure drop, ΔP). The conditions which result in cavitation within the injector and the corresponding effects on mass flow rate have been studied previously by the authors, a detailed description of which can be found in Refs. 5 and 6. This work is essentially a follow-on to the two aforementioned studies which will be referred to repeatedly herein with regard to the effects of cavitation on mass flow rate with an emphasis on the application to the complex problem of combustion instability.

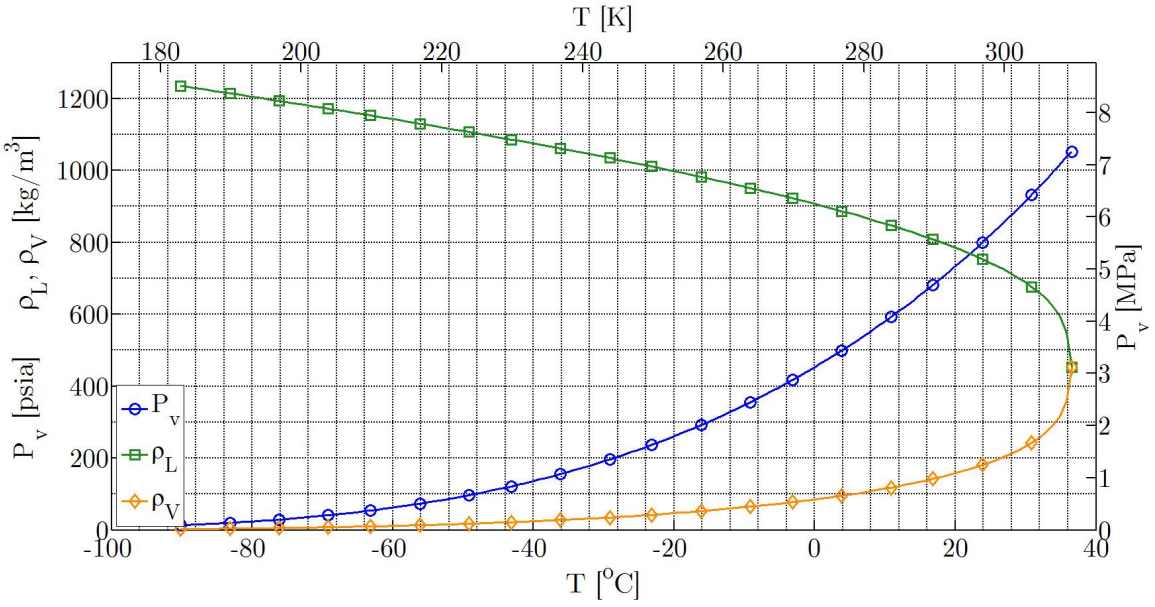

Figure 1. Vapor pressure, liquid density, and vapor density of saturated N_2O vs. temperature. The data used to produce this plot was calculated using REFPROP[3,4].

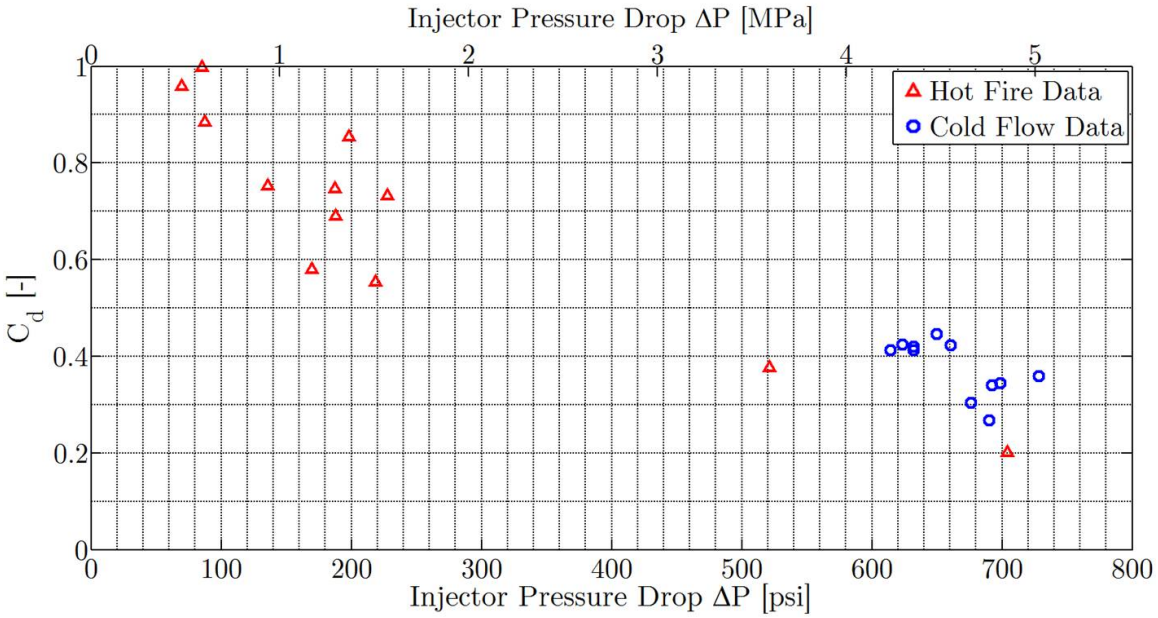

Figure 2. C_d vs. injector pressure drop ΔP for injectors used in hot fire and cold flow tests with N_2O in the Peregrine Sounding Rocket Program (adapted from Ref. 7).

Combustion instability is widely considered one of the most challenging problems to overcome in the development of a new or modified rocket propulsion system. Combustion instability is the term used to describe the undesired and often violent pressure and thrust oscillations that can occur during operation of chemical rockets. The occurrence of combustion instabilities in rocket operation can result in extreme vibrational loading which can cause damage not only to the payload, but to the rocket structure itself. Combustion instabilities also generally result in off-nominal performance of the combustion process and can potentially lead to the destruction of the combustion chamber. Throughout the history of rocket development, a significant body of work has been focused on the understanding and suppression of combustion instability modes in liquid and solid rocket programs. This type of work has involved both a great deal of modeling effort as well as extensive experimental test campaigns in order to eliminate combustion instabilities. Still, there have not been sufficient advances in the fundamental understanding of combustion instabilities to allow for accurate prediction of their onset characteristics and effects. Since there has been so little development in the field of hybrid rocket propulsion over the years as compared to liquid and solid rockets, the understanding of combustion instabilities in hybrids is even less complete. For this reason, some hybrid rocket development programs run into delays and spiraling costs during efforts to achieve sufficiently stable operation.

II. Peregrine Hybrid Sounding Rocket

The Peregrine Sounding Rocket program is a joint effort between Stanford University, NASA Ames Research Center in Mountain View, CA and Space Propulsion Group, Inc., a private rocket development company based in Sunnyvale, CA. The goal of this program is to develop and demonstrate the advantages of the so-called liquefying fueled hybrid rocket technology. The theory and benefits of using liquefying fuels, such as paraffin wax, are outlined in Refs. 8-10. To this end, a single stage sounding rocket is currently under development, capable of lifting a 5 kg payload to the edge of space (100 km). This rocket uses paraffin wax as the fuel and nitrous oxide as the oxidizer. The goals with regard to the actual hybrid rocket propulsion system to be developed for this vehicle were to achieve both stable and efficient combustion throughout the duration of the burn (combustion chamber pressure fluctuations less than ± 5% of the mean and average c^* efficiency greater than 95%). Detailed descriptions of the proposed flight vehicle architecture and early developmental testing of the Peregrine Sounding Rocket can be found in Refs. 1, 6, 7, and 11. However, this work will only focus on the most recent results from a heavyweight ground testing facility designed for developmental testing.

A. Heavyweight Ground Testing Combustion Facility

A heavyweight ground testing combustion facility was developed with the goal of achieving stable and efficient combustion before advancing to the development of flight weight hardware. The internal geometry of this heavyweight combustion facility was intentionally designed to be similar in the overall design of the proposed final flight weight motor. The combustion chamber was built with a thick walled steel pipe and flange design. A cross-section of the heavyweight combustion facility is shown in Fig. 3 with some details of the pipe and flange construction.

Ground testing was performed with both the combustion chamber and a heavyweight oxidizer tank held horizontally. In order to ensure liquid delivery of nitrous oxide with the tank in a horizontal position, a custom eductor, or siphon tube was included at the exit of the oxidizer tank, which acts to position the start of the feed line near the lowest point of the tank. In order to provide adequate initial thrust, the oxidizer tank will operate in a helium-augmented blowdown mode, meaning that before the burn, the nitrous oxide will be pressurized (or supercharged) with helium. However, no on-board pressurization system is planned for the flight vehicle (therefore the tank pressure will not be held constant). The maximum expected operating pressure in the tank is 1000 psia (6.89 MPa). The oxidizer leaves the tank and passes through a 2 inch (5.08 cm) diameter feed line, which houses a pneumatically actuated full port isolation ball valve. This feed line provides oxidizer to the fore end of the combustion chamber, ending at the injector plate. Ignition is provided by solid propellant igniters that protrude into the fore end of the combustion chamber.

To date, approximately 15 tests have been performed in the heavyweight combustion facility (5 cold flows, 10 hot fires). Fig. 4 shows a still image captured during testing in the heavyweight combustion facility for a recent hot fire test.

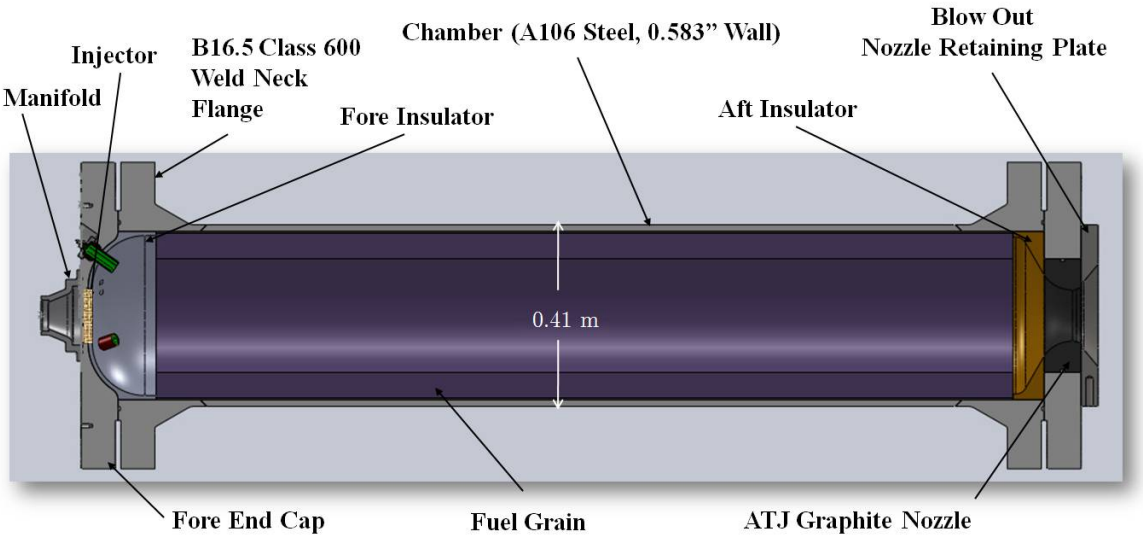

Figure 3. Cross-section model of the Peregrine heavyweight combustion facility chamber.

B. Ground Testing Combustion Instabilities

Unfortunately, the first tests in the Peregrine heavyweight combustion facility exhibited significant combustion instability problems. This section will present chamber pressure data for two of the early tests in this facility. A discussion of the corresponding combustion instabilities that are observed is included, and will serve as the motivation for the work presented in Section III.

Throughout the rest of this work, when presenting test data from the Peregrine heavyweight combustion facility, the actual test numbering used by the Peregrine program will be quoted. The purpose of this is to minimize confusion should the totality of the Peregrine test data be published in the future. The results from each test will be described by presenting the following data:

- Chamber pressure time-histories
- Chamber pressure frequency content (FFT)
- Oxidizer temperature (for reasons to be discussed in Section III).

1. Peregrine Test E2

Test E2 was the first operationally successful hot fire test achieved in the heavyweight combustion facility. The full duration of the proposed Peregrine flight burn is approximately 18 seconds. However, because Test E2 was a development burn, the duration was limited to 5 seconds. The temperature of the nitrous oxide used in this test was approximately 13.5 ^oC (286.7 K) throughout the duration of the burn. Fig. 5 shows the combustion chamber pressure time-history for this test. It is obvious that this test exhibited extremely unstable combustion, with the peak-to-peak amplitude of the chamber pressure oscillations approaching 100% of the mean value over large portions of the test. This is obviously unacceptable for a launch vehicle, even of the sounding rocket variety, and the focus of the Peregrine program was placed squarely on eliminating these instabilities. In order to get a better sense of the character of these chamber pressure oscillations, Fig. 6 is included which zooms in on the data in the time domain (x-axis). The scale for the chamber pressure signal (y-axis) is kept constant, not only for these two plots, but for all of the Peregrine chamber pressure plots presented for the remainder of this work. This is done in order to make comparisons of motor performance from one test to another more straightforward. The point in time for the zoomed in plot was chosen in order to demonstrate that the character of the oscillations changes throughout the test. It can be seen from the zoomed in plot that oscillations are occurring at multiple frequencies. In the first half of the data shown in Fig. 6, it can be seen that there is fairly regular low frequency oscillation, with higher frequency oscillations superposed over that signal

Figure 4. Still photo from hot fire testing in the Peregrine heavyweight combustion facility.

(with the peak to peak amplitude of the oscillations almost equal). The second half of the zoomed in data shows a shift in the character, with the higher frequency oscillation amplitude increasing significantly, to the point where the low frequency oscillations are not clearly visible.

While it is useful to examine this type of data in this zoomed in time window, it is often beneficial to look at the data in the frequency domain instead. This is achieved by applying a type of Fast Fourier Transform (FFT) to the time domain data, the details of which can be found in Ref. 12. In essence, this process involves breaking down the time domain data into a summation of simple sinusoidal signals at different frequencies and determining the amplitude of each frequency. This process can be performed on data during different segments of a hot fire test in the time domain, resulting in the display of the frequency content of the chamber pressure signal over time. This type of data presentation is sometimes referred to as a spectrogram. This process does require "windowing" the data to determine, at each point in time during the burn, how many samples from the data should be used to calculate the frequency information. For all of the spectrograms included in this work, the window length is chosen as 1 second. All of the data is collected at 5000 Hz (per channel), therefore the window length is 5000 samples. These windows are usually overlapped to provide a sufficient number of time points in which to plot the frequency content. However, the actual resolution with respect to time is dependent on the length of the windows chosen (the longer the window, the more data is being used from surrounding points in time). The choice of 1 second FFT windows was made in order to sufficiently resolve the relatively low frequency oscillations which will be seen in some of the test results.

Fig. 7 shows the spectrogram content of the chamber pressure signal from Test E2 plotted over the duration of the burn. It can be seen that there is strong activity around 200-210 HZ, which becomes especially coherent during the second half of the test. This frequency corresponds to the 1st longitudinal acoustic mode of the combustion chamber (acoustic resonance combustion instabilities will be discussed briefly in Section III). It can also be seen that there is a significant level of frequency content down in the 10-25 Hz range. This activity is less coherent, and seems to fade after the first half of the burn. Up to this point in testing, this data was not enough to determine the cause of the low frequency response. In all of the spectrograms that are presented, there is always a strong response near 0 Hz. This is reflective of the fact that the mean value of the signal is shifting over time. This part of the data can be ignored.

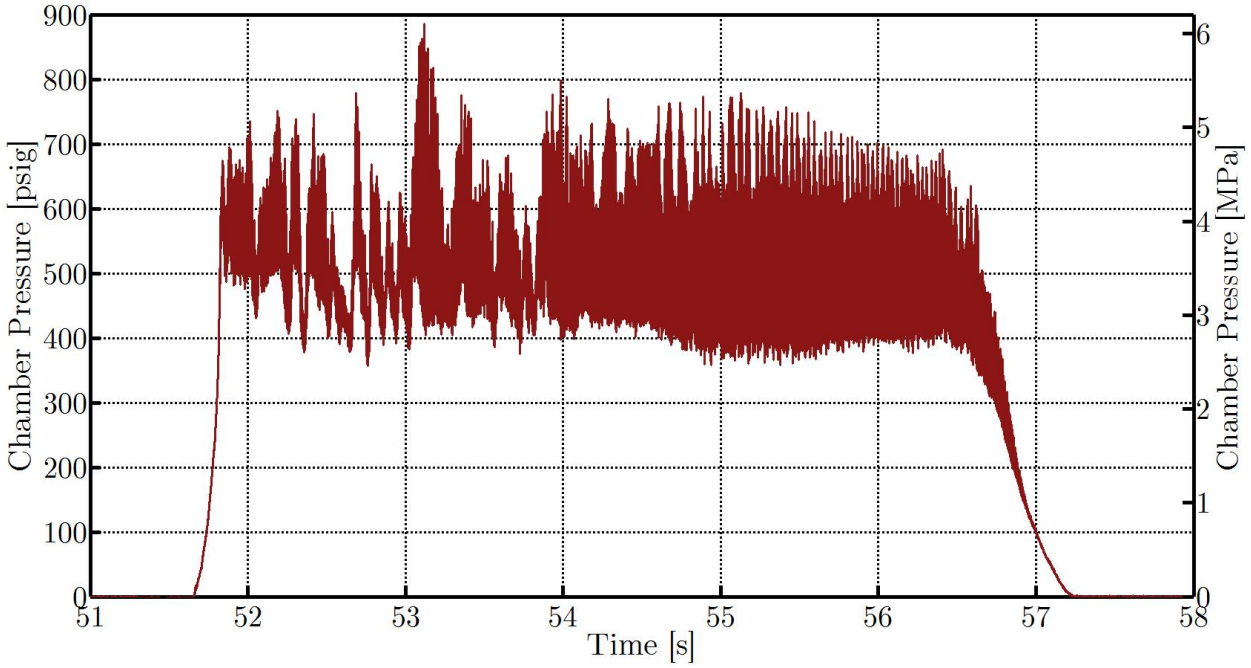

Figure 5. Chamber pressure time-history for Test E2 in the Peregrine heavyweight combustion tests facility with $T_{ox} \approx 13.5\,^{o}C$ (286.7 K).

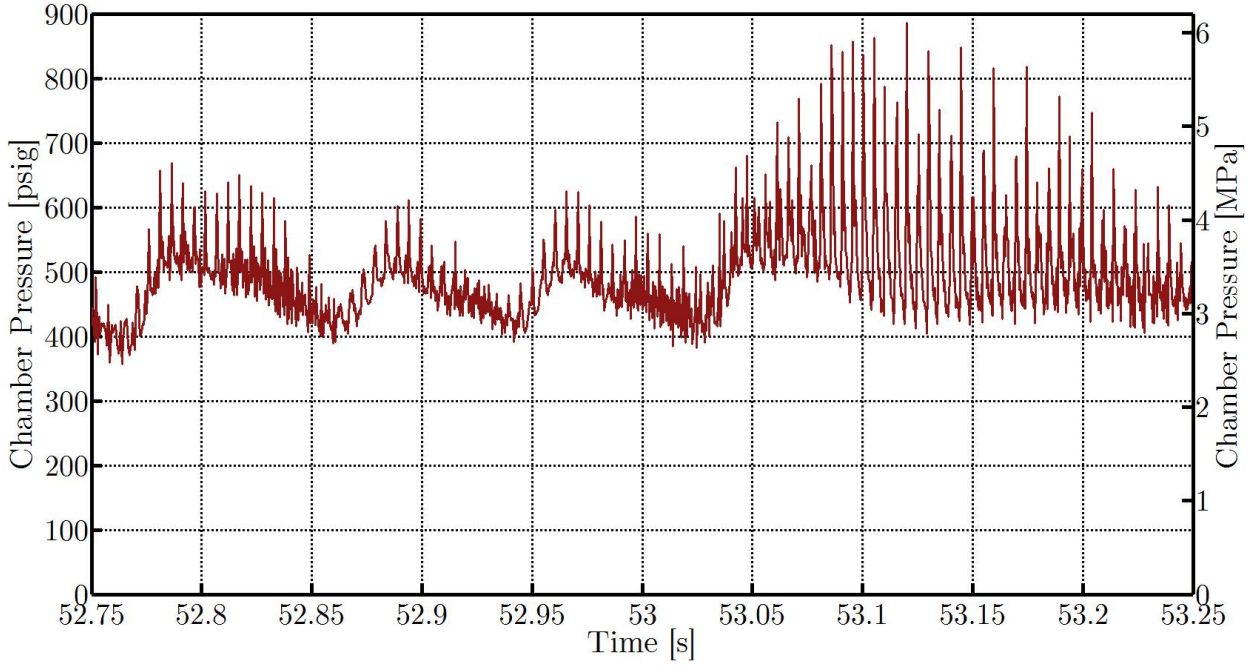

Figure 6. Zoomed in chamber pressure time-history for Test E2 in the Peregrine heavyweight combustion tests facility with $T_{ox} \approx 13.5\,^{o}C$ (286.7 K).

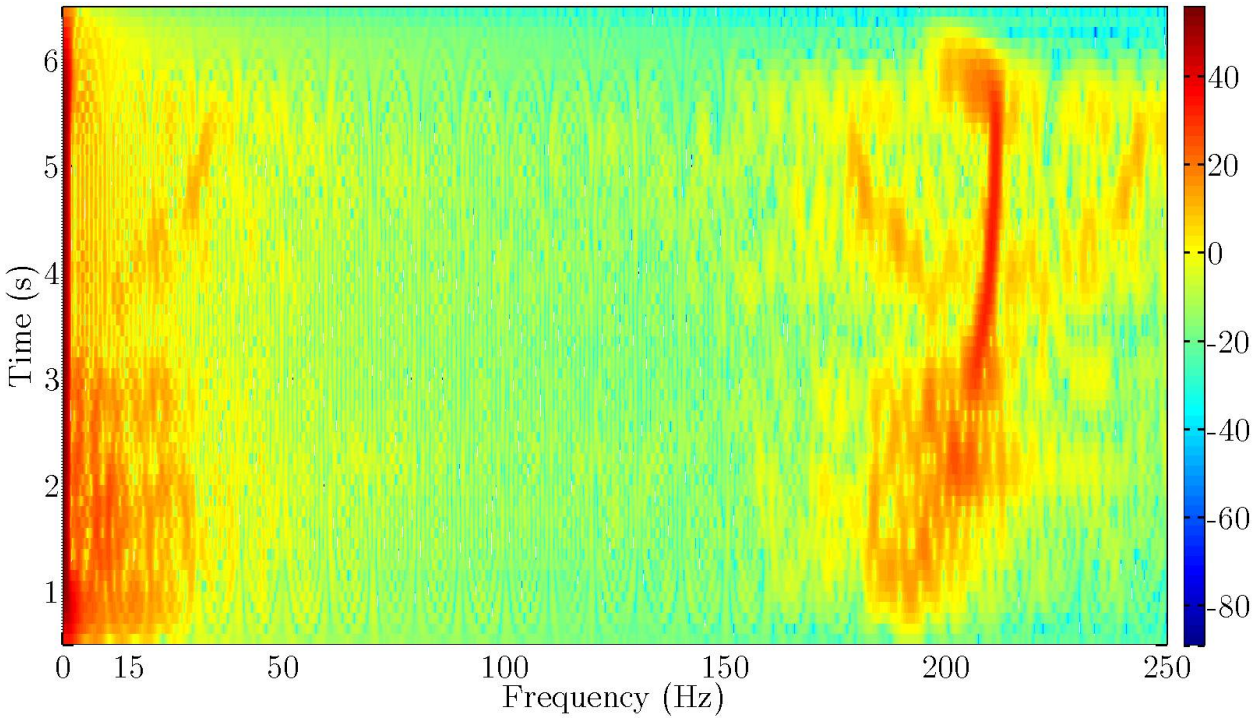

Figure 7. Chamber pressure signal frequency content (FFT) for Test E2 plotted over the duration of the burn with $T_{ox} \approx 13.5\,^{o}C$ (286.7 K). Color is proportional to the power spectral density of the chamber pressure signal.

2. Peregrine Test E3-2

Over the course of the Peregrine tests following Test E2, a variety of changes were made to the design, including changes to the internal combustion chamber geometry. The details of these changes will not be discussed here, but Test E3-2 is a good representation of the motor operation after these changes. Based on how this test fits in with the topic and scope of this work, the conditions and geometry during this test can be treated as a baseline. To state this explicitly, Test E3-2 consisted of the baseline chamber geometry, and used the baseline oxidizer temperature which will be defined as $14.5\,^{o}C$ (287.7 K). This test was also a 5 second developmental burn. Fig. 8 shows the pressure time history for Test E3-2, with the zoomed in data shown in Fig. 9.

It can be seen from Fig. 8 that there were significant improvements in the combustion stability from Test E2 to Test E3-2. However, while the overall character of the two tests looks very different when examined in Fig. 8, the zoomed in data actually shows a surprisingly similar character. Again there are low frequency oscillations with high frequency acoustic content superposed. However, the major difference between the tests is the significant reduction in the amplitude of the acoustic instability pressure oscillations, specifically during the first half of the test. The result is a very coherent low frequency, highly sinusoidal response during the first 2 seconds of the test. This can be seen clearly in the spectrogram shown in Fig. 10. The 15 Hz signal starts off very strong at approximately 110-120 psi (0.76-0.83 MPa) peak-to-peak amplitude and remains throughout the burn, but becomes less coherent and drifts in frequency during the second half of the test, as the acoustic instability grows on top of it. The acoustic instability can also still be seen clearly in the spectrogram, though the relative amplitude has decreased significantly (actually to levels below that of the low frequency mode in the beginning of the test), and is also less coherent than in Test E2. It was with this data that the Peregrine team was able to diagnose the cause of low frequency instability. Due to its highly regular, sinusoidal nature, comparisons with data in the literature pointed to a phenomenon termed the feed system coupled instability. This mode of combustion instability will be described and discussed in detail in Section III, and its suppression will be the focus of the rest of this work.

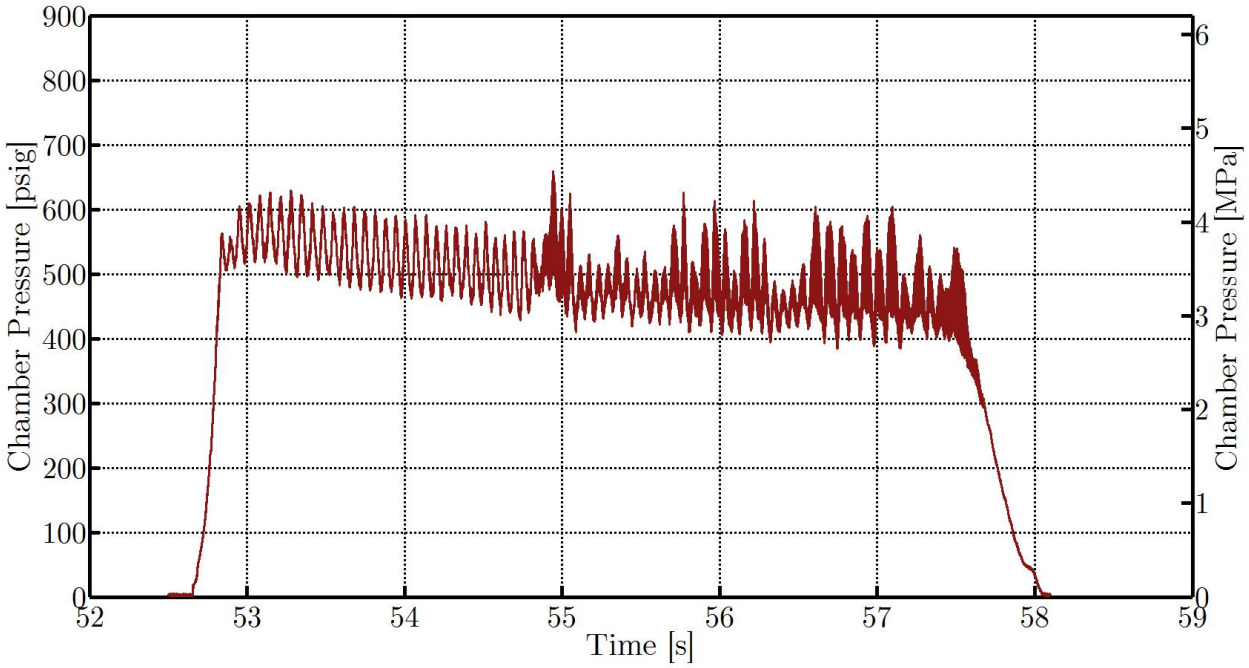

Figure 8. Chamber pressure time-history for Test E3-2 in the Peregrine heavyweight combustion tests facility with $T_{ox} \approx 14.5\,^{o}C$ (287.7 K).

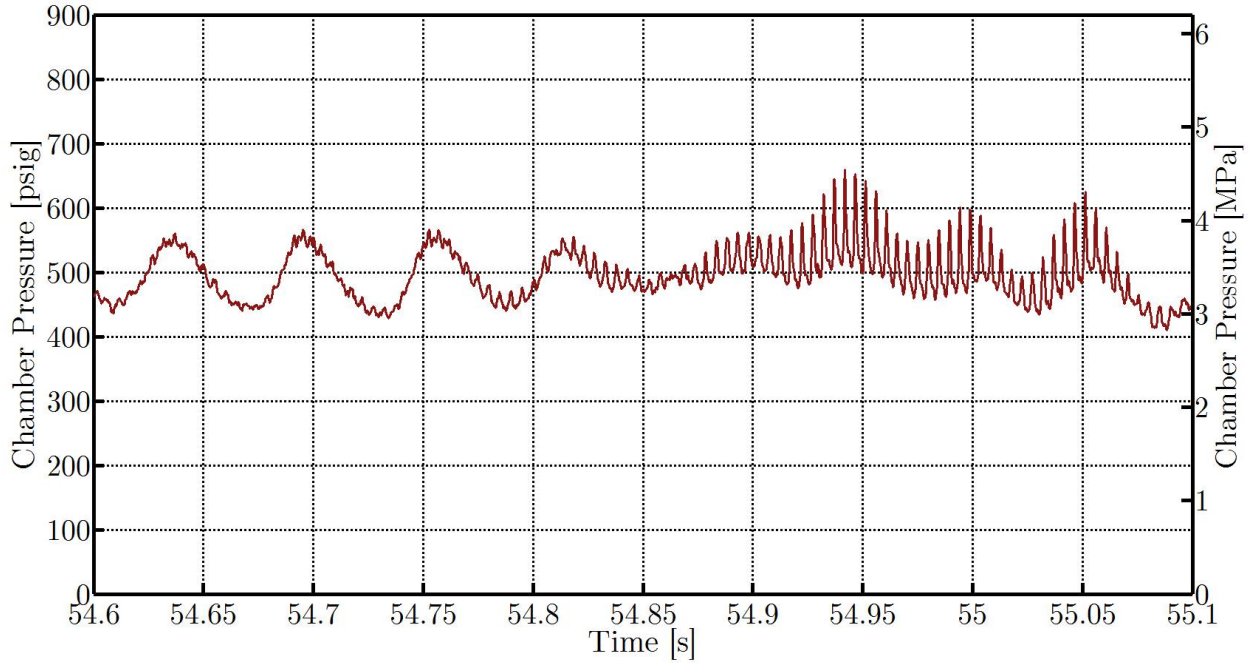

Figure 9. Zoomed in chamber pressure time-history for Test E3-2 in the Peregrine heavyweight combustion tests facility with $T_{ox} \approx 14.5\,^{o}C$ (287.7 K).

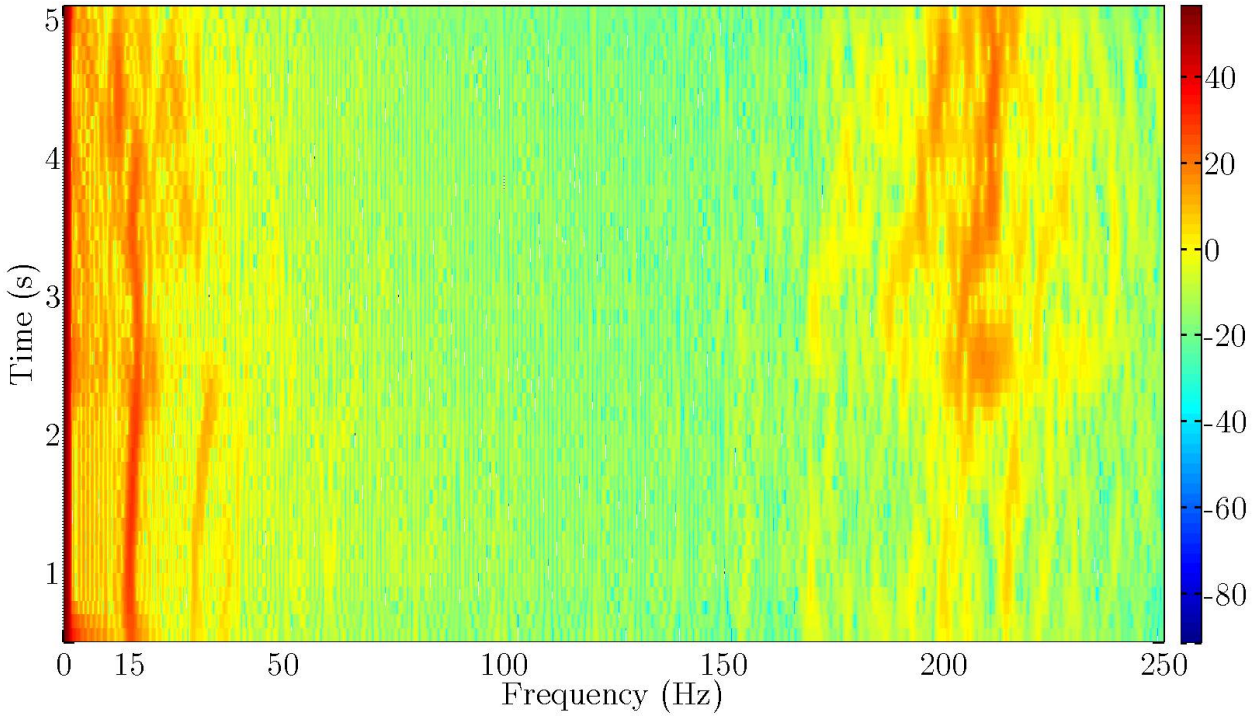

Figure 10. Chamber pressure signal frequency content (FFT) for Test E3-2 plotted over the duration of the burn with $T_{ox} \approx 14.5\,^{o}C$ (287.7 K). Color is proportional to the power spectral density of the chamber pressure signal.

III. Feed System Coupled Combustion Instability

Combustion instability is one of the most commonly encountered problems in the development and testing of rocket propulsion systems, including hybrids. Large amplitude chamber pressure and thrust oscillations often accompany combustion instabilities, resulting in increased vibrational loading, possible structural damage, and on rare occasions catastrophic system failure. As described in Ref. 7 and shown in Section II, progress of the Peregrine Sounding Rocket program has been hampered by combustion instability problems for years. This section will give a brief background into some of the combustion instability modes that are observed in hybrid rockets, with a focus on those instabilities related to the oxidizer feed system. A simple, yet powerful solution to the so called feed system coupled instability is described, and results from a series of Peregrine hot fire tests are presented which verify the effectiveness of this solution.

A. Classification of Combustion Instabilities

Hybrid rocket instabilities can generally be split into two groups:

- High frequency (acoustic instabilities)
- Low frequency (nonacoustic)

High frequency acoustic instabilities are common in all types of rockets. These instabilities form when a there is resonance between energy release from the combustion process and the natural acoustic modes of the combustion chamber internal geometry, or cavity. Combustion chambers can exhibit many natural acoustic modes, often lumped into one of three types: radial, tangential and longitudinal. These designations describe the directional orientation of the pressure waves that form within the chamber, a description of which can be found in Ref. 13. The 1st longitudinal mode (accompanied by its harmonics the 2nd, 3rd longitudinal modes, etc.) is often observed in hybrid rocket motors, and corresponds to pressure waves set up in the axial direction, between the fore end of the combustion chamber and the nozzle contraction at the aft end. The frequencies of the natural modes can be estimated by Eq. (1):

$$f = \frac{a}{l} \tag{1}$$

where f is the frequency of the natural mode, a is the effective average sound speed of the gas within the chamber, and l is the wavelength of the natural mode, which depends on the chamber geometry. Longitudinal modes generally set up as a half-wave, meaning the wavelength is generally twice the axial length of the internal combustion chamber cavity [14]. Informally, the delineation between the high frequency and low frequency combustion instabilities is located at approximately the frequency of the first longitudinal acoustic mode. A variety of methods for the damping of acoustic instabilities have been extensively studied in both the liquid and solid rocket industries, such as Helmholtz resonating cavities in liquid rockets, and the addition of solid particulate to the flow flied in solid rockets [15]. Therefore, acoustic instabilities are not a focus of this work, but will be addressed again briefly in Section III.C.

Two different nonacoustic low frequency instabilities are often observed in hybrid rockets and receive the most attention. The first of these oscillatory behaviors is intrinsic to the interactions between turbulent boundary layer combustion and chamber fluid dynamic behavior. A detailed description of the intrinsic low frequency hybrid rocket instability is provided by Karabeyoglu et al. and is accompanied by the development of a model capable of predicting its frequency [16]. The second common low frequency response is known as feed system coupled instability and will be the focus of the rest of this work due to its inherent relevance to the topic of injectors.

B. Suppression of the Feed System Coupled Instability

Feed system coupled instabilities have been studied extensively in the liquid rocket industry, and have been successfully modeled for a range of engine designs and operating conditions [17]. These instabilities are typically characterized by highly regular, sinusoidal pressure oscillations which are caused by hydrodynamic communication between the combustion chamber and feed system, predominantly observed in systems utilizing liquid oxidizer. Work by Karabeyoglu et al. provides an overview of the feed coupled instability as it pertains to hybrid rockets, and describes a model for predicting its transient behavior [18]. As described in the aforementioned work, the mechanisms that contribute to feed system coupling are:

- Combustion and/or vaporization delay
- Oxidizer flow rate that is dependent on chamber pressure
- Compressibility of fluid in the feed system

Extensive details of the theory and modeling presented by Karabeyoglu et al. can be found in Refs. 6 and 18. The results from the treatment of the feed system coupled instability model presented by Karabeyoglu et al. result in four main suggestions for the design hybrid rockets when trying to avoid the possibility of feed system coupled instability [18]:

- Minimize characteristic oxidizer vaporization delay time (promote rapid vaporization)
- Minimize characteristic feed system pipe response delay time (decrease compressibility within and/or shorten feed system upstream of the injector)
- Design for high injector pressure drop ΔP under nominal motor operation
- Use an isolation element if possible (removing the dependence of oxidizer flow rate on chamber pressure)

As described above, there are a variety of methods that can be employed in an attempt to eliminate feed couple instabilities in hybrid rocket motors. However, the implementation of these techniques are not always practical, and do not guarantee stable operation. For example, due to design constraints, it may not always be possible to shorten the feed system, especially for ground testing setups. Additionally, system constraints can limit the amount of injector pressure drop ΔP that can be achieved, such as maximum allowable working pressures in the feed system, or minimum required combustion chamber pressures. For this reason, this section will focus on the use of isolation elements in the feed system. The mass flow rate of traditional liquid oxidizers through the injector is usually dependent on both P_1 and P_2, the pressure upstream and downstream of the injector respectively. In order to achieve a mass flow rate that is independent of chamber pressure, an isolating element, such as a cavitating venturi is often placed in the feed system upstream of the injector. This has been shown to successfully minimize or completely eliminate feed system coupled instabilities in hybrid rockets [19,20].

1. Cavitating Venturis

The function of a cavitating venturi is to fix, or limit the mass flow rate of a liquid. A standard venturi tube as described in most elementary fluid mechanics courses generally consists of a converging section, a throat section which exhibits the minimum cross-sectional area, and a diverging section. Based upon the Bernoulli equation, as a liquid passes through the converging section, the flow velocity increases and the static pressure decreases. At the throat of the venturi, the flow velocity will be at a maximum, and the static pressure at a minimum. As the flow leaves the throat and passes through the diverging section, the flow velocity decreases and the static pressure increases. When the minimum throat pressure in a venturi is above the vapor pressure of the liquid, only liquid flow exists throughout the flow path. A schematic describing this mode of operation is shown in Fig. 11a. However, cavitating venturis are designed such that at a certain mass flow rate, the minimum pressure at the throat of the venturi is at or below the vapor pressure of the liquid, at which point the liquid starts to vaporize or cavitate near the throat wall. This introduction of vapor bubbles acts to partially block the passageway, and prevents an additional increase in mass flow rate due to any reduction of the downstream pressure (this vapor bubble formation may also occur at different minimum throat pressures due to the desorption of dissolved gases within the liquid). A schematic describing the cavitating mode of operation is shown in Fig. 11b. Changes in upstream pressure can still affect the mass flow rate through the cavitating venturi, and the point at which the venturi begins to cavitate.

Cavitating venturis are often used in liquid rockets to fix the mass flow rate through a liquid propellant feed system. They are generally located upstream of the propellant injector in the main propellant transfer piping. Cavitating venturis are often implemented to simply establish propellant mass flow rates that are insensitive to changes in the downstream pressure. This type of application of the cavitating venturi is described in detail in Ref. 21. In some cases, this effect is utilized in an effort to eliminate or reduce certain types of combustion instabilities feed system coupled instability. When used in this fashion, the cavitating venturi is often described as an isolating element as described above, with the intent of isolating the parts of the feed system and tank upstream of the cavitating venturi from changes in pressure downstream of the cavitating venturi.

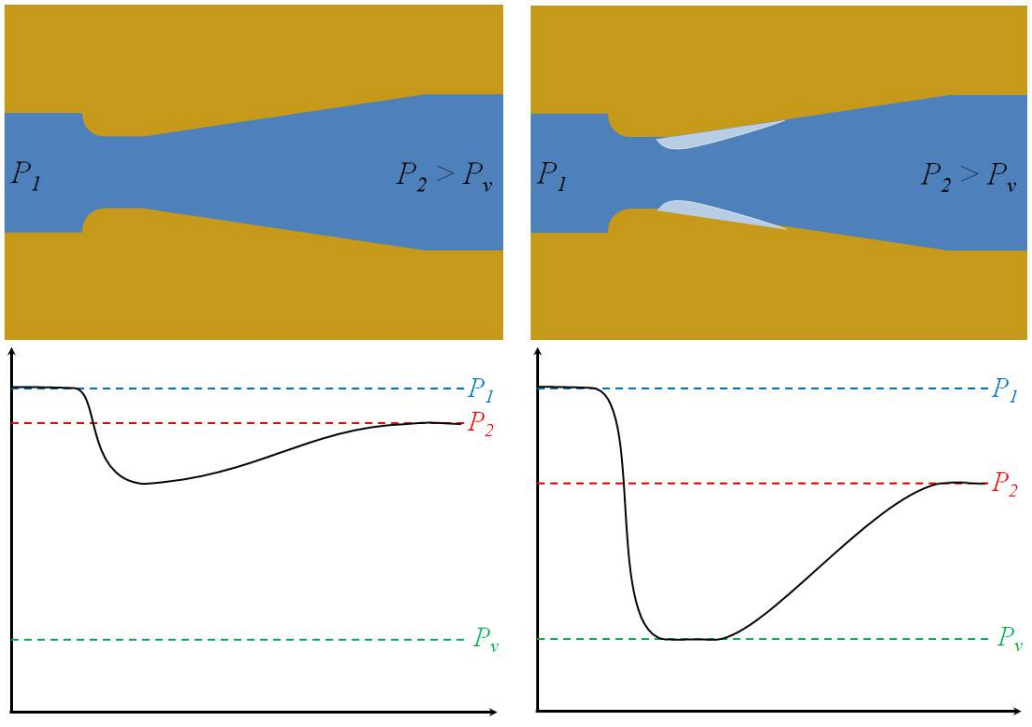

Figure 11. Schematic of the cavitating venturi in (a) non-cavitating operation and (b) cavitating operation.

2. Injector as an Isolating Element

For many traditional rocket propellants such as liquid oxygen (LOX, O2), isolation is successfully achieved through the use of a standard propellant injector and a cavitating venturi operating in concert. The cavitating venturi is located in the main feed system pipe, upstream of the injector. This results in the formation and collapse of vapor bubbles in the main feed line. For systems using nitrous oxide, it can be hazardous to operate with nitrous oxide vapor in the feed system upstream of the injector due to the increased likelihood for an explosive decomposition reaction as outlined in Ref. 22. Further, due to local high temperatures associated with bubble collapse, a possible ignition source exists within the feed system that could lead to this type of decomposition explosion. Therefore, the use of a cavitating venturi in the feed system is potentially problematic for nitrous oxide based hybrid rockets, and will not be considered here. Fortunately, some of the cold flow studies presented by the authors in earlier work described in Ref. 5 identify a potential alternative to the cavitating venturi as a feed system isolating element. As described in Ref. 5, when the pressure downstream of the injector falls sufficiently below the oxidizer vapor pressure, the mass flow rate not only reaches a maximum but becomes independent of the downstream pressure. It should be noted that this has been demonstrated for both large and small values of orifice L/D, however for smaller L/D injectors, critical flow within the injector element does not occur until downstream pressures much lower than P_v are achieved as compared to that of large L/D orifices. Just as with the cavitating venturi, if the mass flow rate is "choked" by the injector element there is no longer a mechanism for hydrodynamic coupling between the combustion chamber and the feed system.

To assist in predicting the conditions necessary for this type of mass flow rate insensitivity, the data from Fig. 21 in Ref. 5 is examined. Fig. 12 consists of mass flow rate performance data for a sample nitrous oxide injector plotted against the ratio of downstream chamber pressure to the oxidizer saturation pressure (P_2/P_v). Details of the cold flow test apparatus used to obtain this mass flow rate data as well as and injector design corresponding to this data can be found in Ref. 5. The supercharge is defined here as the instantaneous difference between the static pressure and the vapor pressure of nitrous oxide at any point in the system. The expression for the supercharge pressure upstream of the injector is shown in Eq. (2), where the vapor pressure is evaluated at the local instantaneous temperature (T_1 in this case). This usage of the term is different than in some previous works which define supercharge as the initial pressurization of the oxidizer tank above the vapor pressure, followed by blowdown operation (no continuous pressurization).

$$P^1_{super} = P_1 - P_v\Big|_{T=T_1} \tag{2}$$

It can be observed in Fig. 12 that chamber pressure disturbances occurring well below the vapor pressure of the oxidizer (P_2/P_v less than approximately 0.8 for this particular injector design) should not be accompanied by any deviation in mass flow rate. As the chamber pressure disturbances approach but remain below the vapor pressure, the injector mass flow rate should start to become sensitive to changes in the chamber pressure, even though two-phase flow likely exists to some extent within the injector element to some extent. For chamber pressures above the saturation pressure of the oxidizer, single-phase flow is expected and pressure disturbances in the chamber should be reflected in the injector mass flow rate as predicted by the single-phase incompressible equation.

It is proposed that a hybrid rocket injection scheme can be set up in such a way to leverage the fact that a nitrous oxide injector operating in the critical flow regime can act as an isolating element itself. In this way the injector would serve as an alternative to the cavitating venturi, providing sufficient isolation functionality while avoiding some of the potential hazards associated with the use of a cavitating venturi with nitrous oxide. The following section will describe the application of the proposed solution in an attempt to eliminate the feed coupled instability in the Peregrine Sounding Rocket heavyweight combustion facility.

C. Application to Peregrine Combustion Stabilization

From the results shown in Section II.B, it became clear that the Peregrine heavyweight combustion facility could serve as an ideal test bed for the validation of the proposed solution to the feed coupled instability presented above in Section III.B. The proposed solution requires setting up the heavyweight combustion facility in such a way that during operation, the chamber pressure will always stay at or below approximately 80% of the oxidizer vapor pressure value (for the high L/D injectors associated with the data in Fig. 12). This can be accomplished in one of two ways:

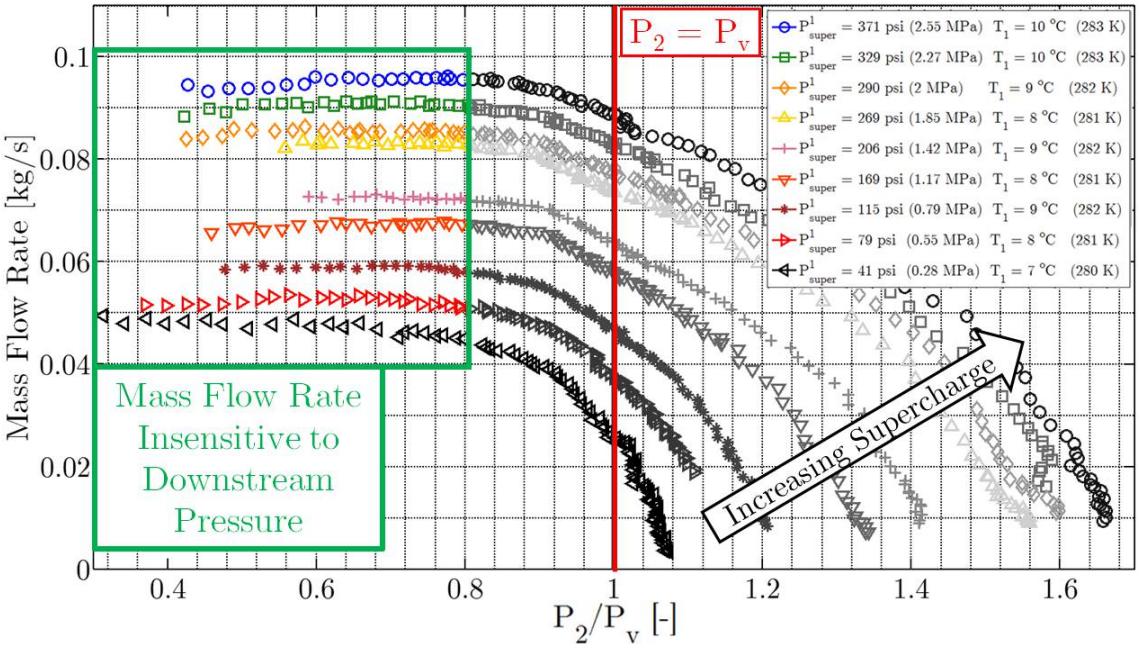

Figure 12. Mass flow rate vs. the ratio of chamber pressure to oxidizer saturation pressure (P_2/P_v). Data is presented for the flow of nitrous oxide through a sample injector over a range of supercharge values. Details of the injector design and the cold flow test apparatus used to make these measurements can be found in Ref. 5.

- Decrease the chamber pressure
- Increase the vapor pressure of the oxidizer

For a variety of reasons, decreasing the chamber pressure is not considered as an option. The main reason for this is that for any rocket system there are usually strict minimum thrust requirements, which depend highly on the chamber pressure that can be obtained. This is certainly the case for the Peregrine Sounding Rocket. For this reason, the attempt to suppress the feed coupled instability in the Peregrine heavyweight combustion facility was constrained to increasing the vapor pressure of the oxidizer. In order to achieve this, it was necessary to increase the temperature of the oxidizer. Recall that the relationship between nitrous oxide temperature and vapor pressure is included in Fig. 1. The operating parameters from Tests E2 and E3-2 are shown in Table 2 in order to give a starting point for the determination of the required oxidizer temperature for further testing. It can be seen that for both of these initial tests, the chamber pressure was well above 80% of the vapor pressure, thus the existence of the feed coupled instability is not surprising. In order to assess the effectiveness of an isolating injector with regards to suppressing the feed coupled instability, a proposed set of Peregrine heavyweight operating conditions were determined, and are shown in Table 2 as well, notably with an oxidizer temperature of 21.0 ^oC (294.2 K). Note that the sole difference between test E3-2 and the proposed test is an increase in the oxidizer temperature of 6.5 ^oC (6.5 K).

Table 2. Operating parameters for Tests E2 and E3-2 with proposed parameters for suppression of the feed system coupled instability.

Parameter	Test E2	Test E3-2	Proposed
T_{ox} , ^oC (K)	13.5 (286.7)	14.5 (287.7)	21.0 (294.2)
P_v , psia (MPa)	629 (4.34)	644 (4.44)	747 (5.15)
$P_{2\,initial\,avg}$, psia (MPa)	~575 (3.96)	~550 (3.79)	~550 (3.79)
$P_{2\,initial\,avg}/P_v$	~0.91	~0.85	~0.74

Before presenting the resulting Peregrine test data, the expected test results using the proposed operating parameters should be discussed. It was expected that the feed system coupled instability should be of smaller amplitude, or be eliminated completely. However, with the reduction of the feed coupled instability, and thus a more steady oxidizer mass flow rate into the combustion chamber, it was predicted that the conditions would be more favorable for the

establishment of the acoustic instability observed in Test E3-2. Therefore, it was expected that with the successful elimination of the feed coupled instability, a stronger and more coherent acoustic mode would be observed. This was the goal of Test E3-4 which will be described below. The resulting plan for the ensuing Peregrine Sounding Rocket heavyweight combustion facility test program was to first attempt to eliminate the feed coupled instability, and then shift efforts to eliminating the acoustic instability only after the feed coupled instability was suppressed.

1. Test E3-4 Results

The operating conditions for Test E3-4 were set to the proposed parameter values listed in Table 2, specifically T_{ox}= 21.0 ^{o}C (294 K) and an expected initial peak chamber pressure of $P_{2\,initia\,avg}$ of 550 psi (3.79 MPa). This test was a 5 second developmental burn. The chamber pressure time-history for test E3-4 is shown in Fig. 13 and Fig. 14, and the results are quite noteworthy. As expected, over the majority of the burn, the amplitude of the low frequency feed system coupled instability was reduced to approximately 10-20 psi (0.07- 0.14 MPa) peak-to-peak amplitude. As predicted earlier, with the reduction of the feed system coupled mode, the acoustic instability was stronger and more coherent, as is clearly visible in Fig. 14. The amplitude of the acoustic instability during this tests starts off at approximately 150 psi (1.03 MPa) peak-to-peak, and is approximately 90 psi (0.62 MPa) peak-to-peak at the end of the test. These exciting results signaled a highly successful demonstration of the use of a critical flow injector as an effective flow isolating element. Since the adoption of this new critical flow injector operating criteria, no tests have resulted in the observation of the feed system coupled combustion instability mode.

It should be noted that during the first 0.3 second of the burn, feed system coupled instability is observed, as is clearly visible in both Fig. 13 and in the spectrogram frequency content of Fig. 15. A long feed system pipe exists between the oxidizer tank and the injector face. The pipe material and the nitrous oxide contained within it are pre-chilled as part of the operating procedure for the heavyweight combustion facility. It is thought that initially cold (lower vapor pressure) nitrous oxide flows through the injector during this initial phase, resulting in the injector not operating under critical flow conditions. Further testing in this facility provided less cooling to the feed line to address this issue.

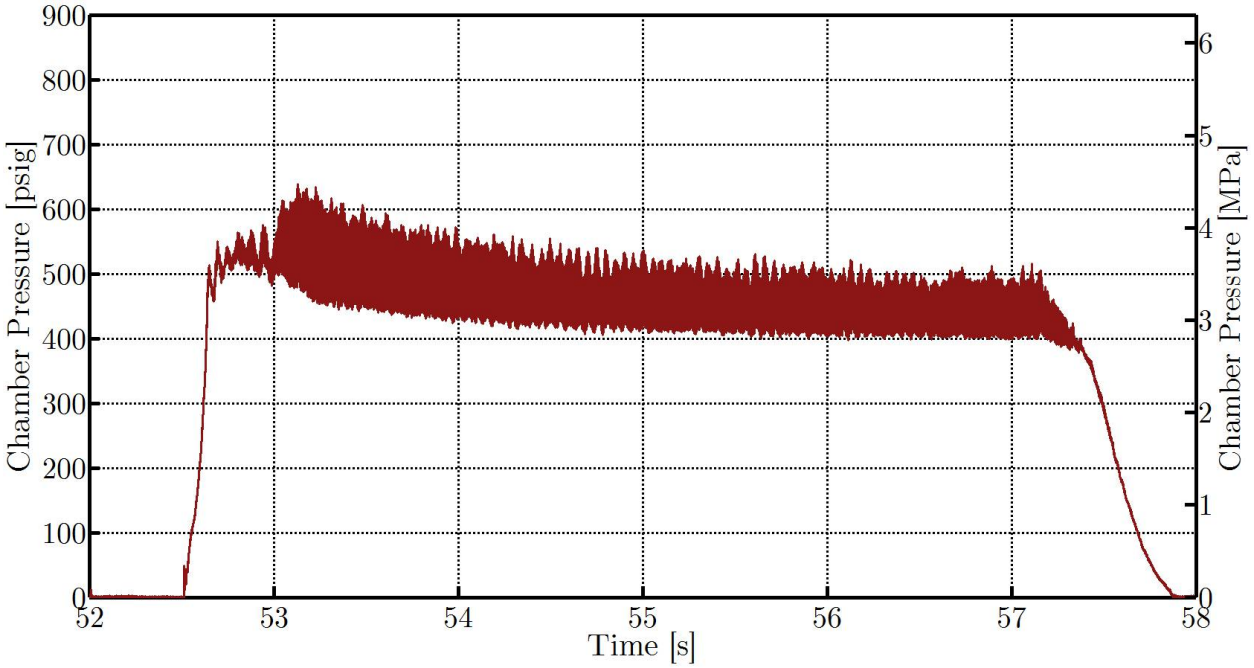

Figure 13. Chamber pressure time-history for Test E3-4 in the Peregrine heavyweight combustion tests facility with $T_{ox} \approx 21.0\,^{o}C$ (294.2 K).

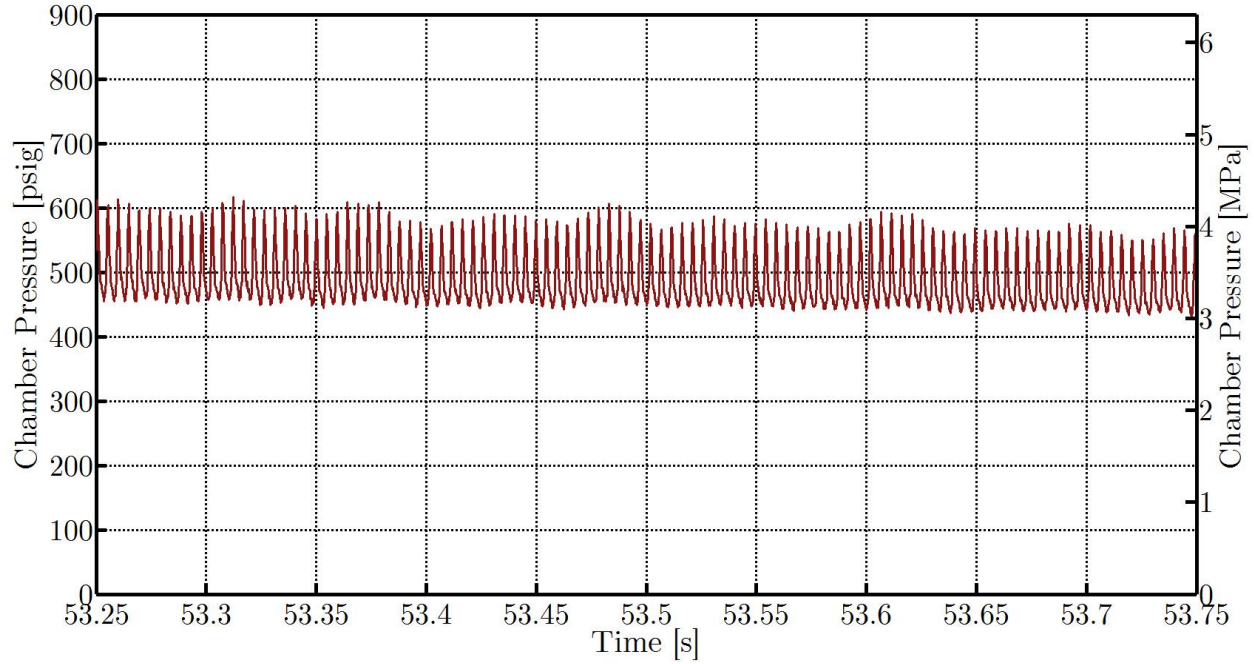

Figure 14. Zoomed in chamber pressure time-history for Test E3-4 in the Peregrine heavyweight combustion tests facility with $T_{ox} \approx 21.0\,^{o}C$ (294.2 K).

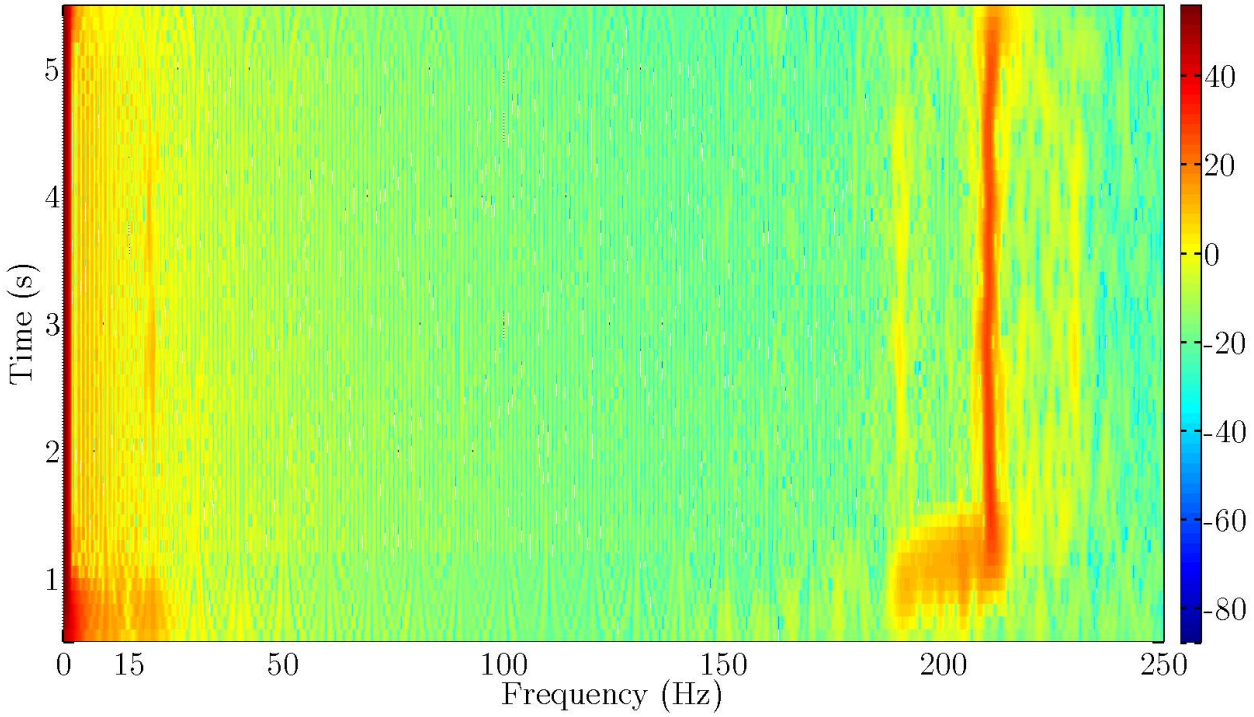

Figure 15. Chamber pressure signal frequency content (FFT) for Test E3-4 plotted over the duration of the burn with $T_{ox} \approx 21.0\,^{o}C$ (294.2 K). Color is proportional to the power spectral density of the chamber pressure signal.

2. Test E4-1 Results

Once the elimination of the feed system coupled instability was achieved, the Peregrine program was able to focus on suppressing the acoustic instability. Over the course of 2 hot fire tests, some relatively simple changes to the configuration of the Peregrine heavyweight combustion facility were made in hopes of damping the acoustic instability observed in Test E3-4. The details of the geometry modification will not be presented here, but the results from the corresponding test (Test E4-1) will be included in order to provide the reader with the current state of the performance achieved in the Peregrine heavyweight combustion facility. Test E4-1 was a longer 8 second burn, using oxidizer at a temperature of 22.5 ^{o}C (295.7 K). As can be seen from Fig. 16 and Fig. 17, the chamber pressure time-history from this test shows that the acoustic instability was damped to such a degree that motor exhibited extremely stable combustion. Again, as shown in Fig. 18, there is a small amount of low frequency activity at the start of the burn around the feed coupled instability mode frequency, which still may be attributed to the feed line chilling procedure (which was in fact scaled back, but not removed completely). Looking closely at Fig. 16 this early low frequency activity can just barely be distinguished. It should be noted that while it may have been possible to remove the acoustic instability first, the success of the Peregrine heavyweight combustion facility test campaign was dependent on the elimination of the feed system coupled instability.

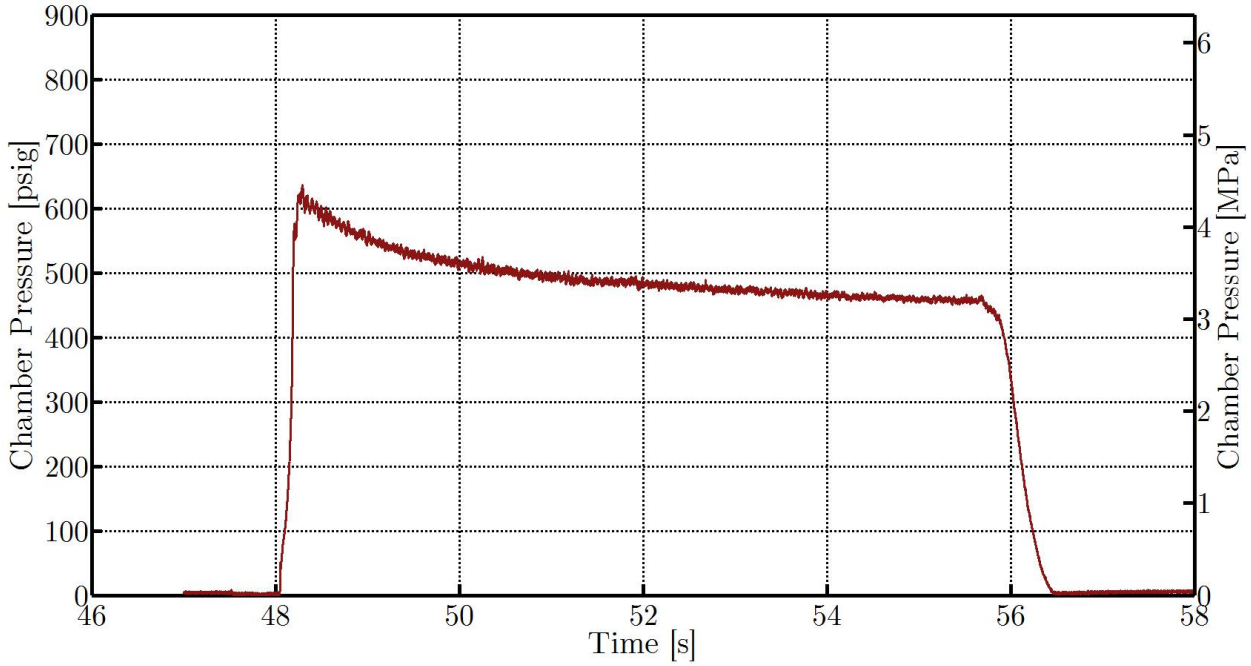

Figure 16. Chamber pressure time-history for Test E4-1 in the Peregrine heavyweight combustion tests facility with $T_{ox} \approx 22.5\,^{o}C$ (295.7 K).

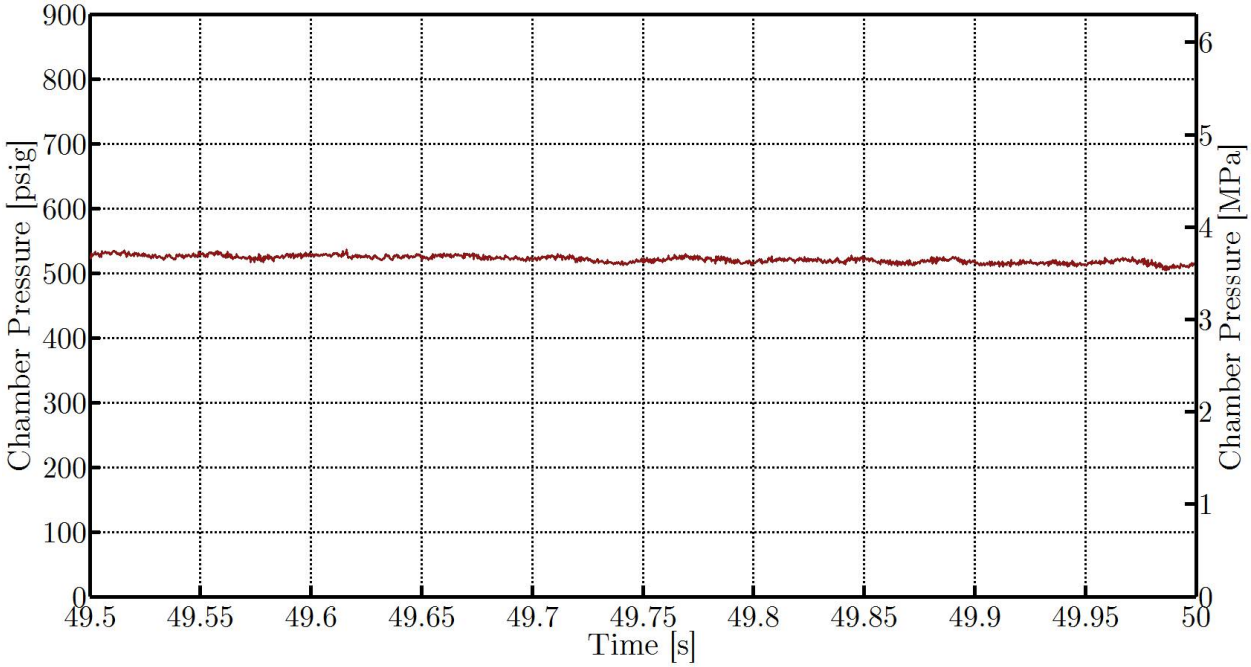

Figure 17. Zoomed in chamber pressure time-history for Test E4-1 in the Peregrine heavyweight combustion tests facility with $T_{ox} \approx 22.5\,^{o}C$ (295.7 K).

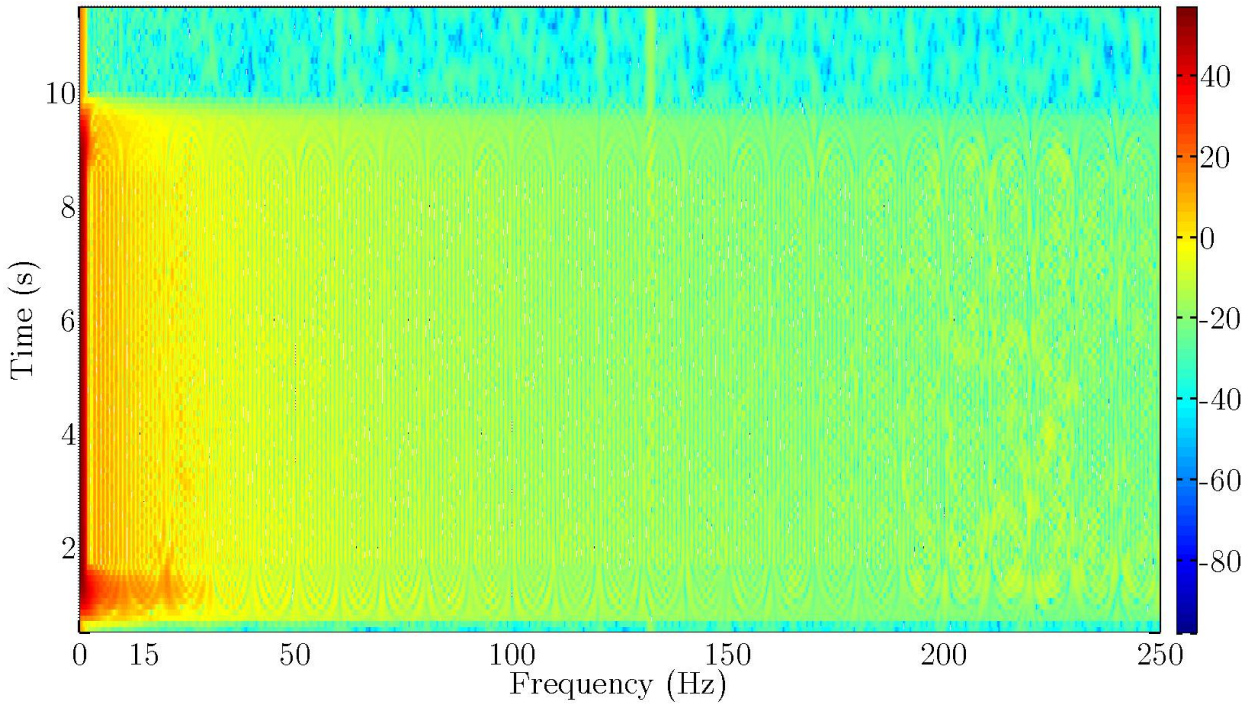

Figure 18. Chamber pressure signal frequency content (FFT) for Test E4-1 plotted over the duration of the burn with $T_{ox} \approx 22.5\,^{o}C$ (295.7 K). Color is proportional to the power spectral density of the chamber pressure signal.

IV. A Novel Hybrid Rocket Injection Scheme

It was shown definitively in Section III that a properly designed injection scheme can result in the avoidance of feed system coupled combustion instabilities in hybrid rocket motors. Specifically, operating a hybrid rocket motor with an injector exhibiting critical flow has been shown to successfully eliminate feed coupled instabilities in full scale hybrid rocket tests. However, the aforementioned criteria used for suppressing feed coupled instabilities does result in certain restrictions on operating conditions and has a negative impact on the performance of the overall rocket system. These drawbacks will be outlined in this section. Fortunately, a novel hybrid rocket injection scheme has been developed which essentially removes the constraints imposed by the criteria presented in Section III, while maintaining the critical flow injector isolation performance. This improvement will be outlined in this section, and the results from a series of cold flow experiments will be presented to serve as a proof of concept.

A. Undesired Consequences of Stabilization Criteria

As described in Section III.C, it is possible to provide resistance to the development of the feed system coupled instability by ensuring that the injector mass flow rate is independent of the chamber pressure. This is achieved for standard oxidizer injectors by setting the chamber pressure sufficiently below the vapor pressure to promote critical two-phase flow through the injector. The exact percentage to which the chamber pressure must be set below the vapor pressure depends upon the design of the given injector and the thermodynamic conditions of the oxidizer supplied to the injector. However, for the high L/D injectors using supercharged nitrous oxide studied by the author, a useful criteria for critical flow is shown in Eq. (3).

$$P_2 < 0.8P_v \tag{3}$$

While the benefits from the use of this criteria can be substantial, there are two main negative consequences of its use:

- Limitations on operating conditions
- Reduction in overall rocket performance (due to mass penalty)

In one form another, the rocket designer is constrained if this criteria is used. If there are operational upper limits on the temperature of the oxidizer being used, there will likely be little flexibility on the choice of chamber pressure. Further, for traditional low vapor pressure oxidizers, this criteria is essentially useless. Additionally, if a minimum chamber pressure is required, oxidizer below a certain temperature cannot be used. Depending on the oxidizer of choice, even with nitrous oxide, this could result in the inability to achieve performance goals. Overall, this criteria can severely restrict the design space for hybrid rockets.

In terms of performance, it is useful to examine the effects of this criteria on the overall mass of the rocket system. As an example, a hypothetical nitrous oxide based hybrid rocket can be considered. Assuming a minimum chamber pressure is required in order to achieve some minimum thrust level, the nitrous oxide temperature will likely need to be set relatively high (as was done for Test E3-4 in Section III.C). This results in an increased oxidizer vapor pressure P_v, which is necessary to ensure critical flow through the injector. However, this requires the storage of oxidizer at a higher pressure, resulting in a thicker walled, thus heavier oxidizer tank. On top of that, it can be seen from Fig. 1 that as the temperature of nitrous oxide is increased, the liquid density can decrease significantly, especially nearing the thermodynamic critical point. This results in an increased volume of oxidizer to store, and a larger tank. With the requirement of a larger, thicker walled oxidizer tank, the impacts on overall ΔV performance can be substantial. This may be fine for some development programs, but unacceptable for others.

For the reasons outlined above, an effort was made to develop a method of oxidizer injection which can operate in the critical flow regime for more arbitrary operating conditions, with regard to both chamber pressure and oxidizer temperature/vapor pressure. The following sections will describe one such method which has been proposed by the author.

B. Improved Isolating Injection Scheme

A new class of rocket propellant injectors has been proposed which allows for operation in the critical flow regime over essentially arbitrary conditions. While this improved injection scheme was conceived of with the use of nitrous oxide in mind, it applies equally as well to the use of traditional, low vapor pressure propellants. This section describes the injection scheme in detail and some important design considerations.

1. Goal

As mentioned previously, the goal in developing this injection scheme was to provide an isolating injector that could perform in the critical flow regime over a broader, essentially arbitrary set of operating conditions. Specifically, these conditions can be outlined as:

- Arbitrary chamber pressure
- Broad range of oxidizer temperatures (vapor pressure)
- All propellants

For example, when using standard injector orifices with nitrous oxide, in order to achieve high chamber pressures, high temperature nitrous oxide must be used. It would be preferred if cold nitrous could be used in order to be stored at lower pressures and with higher density. Additionally, while the bulk of this work has focused on high vapor propellants such as nitrous oxide, an improved injection scheme should provide for isolation using traditional, low vapor propellents as well (such as LOX, kerosene, etc.)

2. Approach

Recalling the description of cavitating venturis in Section III.B.1, it is well known that these can be designed to provide fixed mass flow rates for low vapor pressure propellants over a broad range of operating conditions. Again, these devices are generally located upstream of the injector in the main feed line. This approach is still not considered because it is not suitable for nitrous oxide systems, and additionally there are benefits to collocating the isolating element with the injector. First, avoiding the use of a dedicated cavitating venturi in the feed line results in weight savings, thus improved performance. Second, by collocating the isolating element with the injector, the entire feed

system upstream of the injector will be isolated from the combustion chamber. With a dedicated cavitating venturi, a small portion of the feed system downstream of the cavitating venturi but still upstream of the injector will likely be in hydrodynamic communication with the combustion chamber.

In order to achieve the goals stated in Section IV.B.1, a novel, yet relatively simple approach is proposed. This injection scheme involves designing each individual injector orifice in a similar fashion as that of a cavitating venturi. Specifically, the contour of each injector orifice must have a defined throat and a diverging section, termed the diffuser. A smooth converging section (rounded inlet) is preferable, but not necessary. The proposed injector orifice design provides the functionality of both the standard injector and the cavitating venturi in a single component. It is designed such that under the desired conditions for critical flow, the throat pressure is at or below the vapor pressure of the liquid. A schematic of the cavitating venturi style injector is shown in Fig. 19.

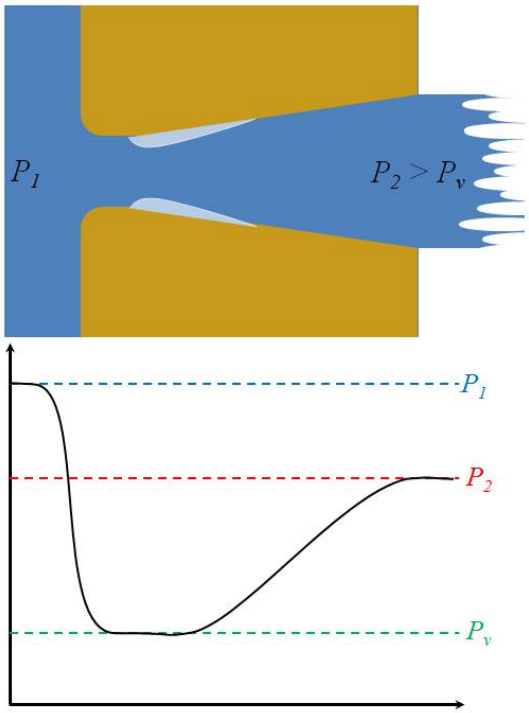

Figure 19. Schematic of the cavitating venturi style injector operating in the critical flow regime.

While the description of the standard cavitating venturi and the cavitating venturi style injector are quite similar, the functionality is actually quite different. Standard cavitating venturis are generally flow limiting devices, in that beyond a certain mass flow rate, cavitation begins, and the mass flow rate can be increased no more. The pressure drop ΔP across a typical cavitating venturi in both the cavitating and non-cavitating regimes is generally not large, and is not the driving force for the mass flow. The driving force for the mass flow rate is the pressure drop across the standard injector that is located downstream of the cavitating venturi in the feed system. On the other hand, the cavitating venturi style injector does exhibit a large ΔP, providing the driving force for the mass flow rate, as well as mass flow rate limiting. Therefore these two factors of the component are linked, thus the design, analysis, and operation of a cavitating venturi style injector is quite different in practice than that of the standard cavitating venturi. For this reason, the next section will provide a sample analysis specific to this new class of rocket propellant injectors.

3. Sample Analysis

In order to demonstrate some design considerations which are unique to this new injection scheme, and example analysis will be provided in this section. The analysis will be carried out in a similar fashion to that of simple single phase incompressible liquid flow rate predictions as described in Ref. 5. This simplified style of analysis is chosen

because it will aid in the understanding of this new class of injectors and their functionality. The assumptions made in this section do not constitute conditions under which the device must operate. On the contrary, this same analysis can be completed without the included assumptions to predict the behavior of this device under arbitrary conditions. This analysis also serves as a guide for the method of selecting the specific geometry of the device in order for it to perform as desired under known operating conditions.

A notional cross-section for one of these injectors is shown in Fig. 20. The actual shape of this cross-section is arbitrary and unimportant, but the cross-sectional areas of the indicated locations are the important information. The features of this injection scheme included for this analysis are the area upstream of the injector, the inlet, the converging section, the throat, and the diffuser section, ending at the injector exit. The analysis starts with conservation of mass throughout the device, under the assumption of steady state operation, resulting in the continuity equation as shown in Eq. (4).

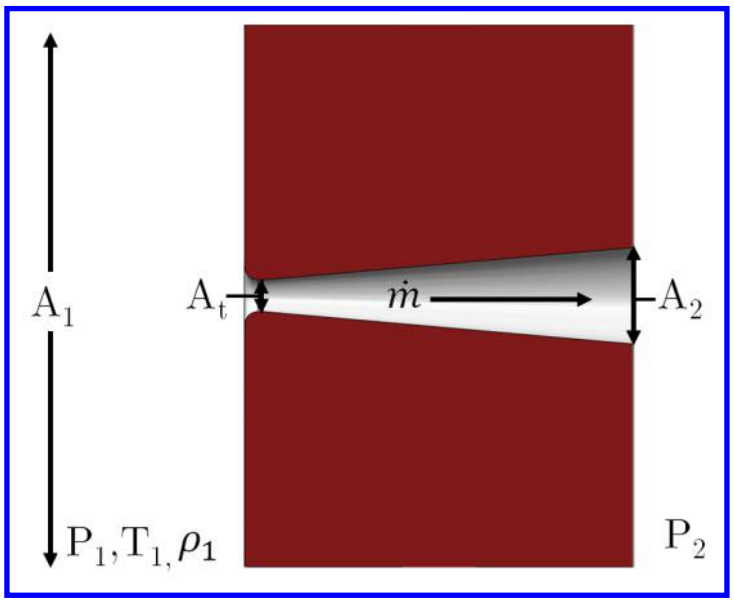

Figure 20. Notional cross-section of the proposed novel injection scheme, with important parameters labeled.

$$\rho_1 u_1 A_1 = \rho_t u_t A_t = \rho_2 u_2 A_2 \tag{4}$$

For this example calculation, it is assumed that the flow is incompressible liquid, thus the density is constant:

$$\rho_1 = \rho_t = \rho_2 = \rho \tag{5}$$

$$\rho u_1 A_1 = \rho u_t A_t = \rho u_2 A_2 \tag{6}$$

$$u_1 A_1 = u_t A_t = u_2 A_2 \tag{7}$$

This results in a list of useful relations which will be called upon later, as shown in Eqns. (8) - (13):

$$u_1 = \frac{A_t}{A_1} u_t \tag{8}$$

$$u_t = \frac{A_1}{A_t} u_1 \tag{9}$$

$$u_1 = \frac{A_2}{A_1} u_2 \tag{10}$$

$$u_2 = \frac{A_1}{A_2} u_1 \tag{11}$$

$$u_t = \frac{A_2}{A_t} u_2 \tag{12}$$

$$u_2 = \frac{A_t}{A_2} u_t \tag{13}$$

Next the Bernoulli equation is employed, again assuming incompressible liquid flow, to calculate the mass flow rate through the injector based on the conditions upstream (location 1) and at the exit of the injector (location 2) as shown in Eq. (14):

$$P_1 + \frac{1}{2}\rho u_1^2 + \rho g_o h_1 = P_2 + \frac{1}{2}\rho u_2^2 + \rho g_o h_2 \tag{14}$$

Assuming that the difference in gravitational potential energy between locations 1 and 2 is negligible, the resulting form can be simplified as in Eq. (15):

$$P_1 + \frac{1}{2}\rho u_1^2 = P_2 + \frac{1}{2}\rho u_2^2 \tag{15}$$

A useful expression for velocity at the exit, u_2, can be found by manipulating this form of the Bernoulli equation and by employing some of the useful relations presented above in Eqns. (8) through (13). This form is shown in Eq. (16):

$$u_2 = \sqrt{\frac{2(P_1 - P_2)}{\rho\left[1 - (\frac{A_2}{A_1})^2\right]}} \tag{16}$$

Using the above relations, the mass flow rate through the injector can be calculated as shown in Eq. (18):

$$\dot{m}_{inj} = \rho u_2 A_2 \tag{17}$$

$$\dot{m}_{inj} = A_2 \sqrt{\frac{2\rho(P_1 - P_2)}{\left[1 - (\frac{A_2}{A_1})^2\right]}} \tag{18}$$

Due to the possible presence of a vena contracta as well as definite frictional losses, the mass flow rate achieved is usually lower than the ideal value as predicted by the equation above. For this reason, an empirically determined discharge coefficient for the injector orifice is included as shown in Eq. (19):

$$\dot{m}_{inj} = C_{d,inj} A_2 \sqrt{\frac{2\rho(P_1 - P_2)}{\left[1 - (\frac{A_2}{A_1})^2\right]}} \tag{19}$$

Now the same process can be repeated as above for the segment of the injector from the throat (location t) to the exit of the injector (location 2). This segment of the injector will be called the diffuser. The expression for the mass flow rate based on the diffuser calculation is shown in Eq. (20). It should be noted that a different discharge coefficient for only the diffuser section is included in this equation.

$$\dot{m}_{diff} = C_{d,diff} A_t \sqrt{\frac{2\rho(P_2 - P_t)}{\left[1 - (\frac{A_t}{A_2})^2\right]}} \tag{20}$$

During steady operation, the mass flow rate through the injector and the diffuser section must be equal to one another, resulting in the equality shown in Eq. (22):

$$\dot{m}_{inj} = \dot{m}_{diff} \tag{21}$$

$$C_{d,inj}A_2\sqrt{\frac{(P_1-P_2)}{\left[1-(\frac{A_2}{A_1})^2\right]}}=C_{d,diff}A_t\sqrt{\frac{(P_2-P_t)}{\left[1-(\frac{A_t}{A_2})^2\right]}} \tag{22}$$

The above equation can be solved for the throat pressure P_t, as a function of a given injector geometry (A_1, A_2, A_t), the upstream and downstream operating pressures (P_1, P_2), and the discharge coefficients for the injector and diffuser section $(C_{d,inj}, C_{d,diff})$, as shown in Eq. (23):

$$P_t=P_2-\left(\frac{C_{d,inj}}{C_{d,diff}}\right)^2\left(\frac{A_2}{A_t}\right)^2\frac{\left[1-(\frac{A_t}{A_2})^2\right]}{\left[1-(\frac{A_2}{A_1})^2\right]}(P_1-P_2) \tag{23}$$

For a specific combination of injector geometry and operating pressures, if the throat pressure P_t is below the vapor pressure of the propellant P_v, it is expected that cavitation/vaporization will be present at the throat. This is the desired operation of the device, and the criterion for operation is simply stated in Eq. (24) and Eq. (25):

$$P_t<P_v \qquad (for\ critical\ flow) \tag{24}$$

$$P_2-\left(\frac{C_{d,inj}}{C_{d,diff}}\right)^2\left(\frac{A_2}{A_t}\right)^2\frac{\left[1-(\frac{A_t}{A_2})^2\right]}{\left[1-(\frac{A_2}{A_1})^2\right]}(P_1-P_2)<P_v \qquad (for\ critical\ flow) \tag{25}$$

Eq. (24) and Eq. (25) constitute the basis of operation for this new class of injector. Under these conditions, the injector will operate in the critical flow regime, providing isolation. However, the injector can be operated outside of the above criteria under conditions where the flow would not cavitate, and no choking or isolation should be expected. It should also be noted that the vapor pressure of the propellant may not remain constant as it passes through the injector. In some cases, the propellant temperature will be dropping as the liquid moves toward the throat of the injector (as described in Ref. 6). In this case, the local vapor pressure at the throat may be lower than the vapor pressure of the upstream propellant. Thus, the value of the throat pressure P_t resulting in mass flow rate choking can be significantly lower than those presented above, depending on the properties of the propellant. Other factors can also significantly affect the onset of mass flow rate choking, such as the fluid existing in a metastable state, especially for propellants existing close to their vapor pressure upstream of the injector. This treatment could be supplemented using a two-phase flow model as described in Ref. 6, but this presentation is not included here, as this analysis is just given as an example to show the necessary considerations for designing an isolating injector of this type. Instead, in order to ensure choking and isolation, a reasonable margin can be chosen between the throat pressure and the known upstream vapor pressure (e.g. $P_t < 0.8P_v$ as described similarly in Section III for standard injectors) as shown in Eq. (26) and Eq. (27):

$$P_t<0.8P_v \qquad (for\ critical\ flow\ with\ 20\%\ margin\ on\ P_v) \tag{26}$$

$$P_2-\left(\frac{C_{d,inj}}{C_{d,diff}}\right)^2\left(\frac{A_2}{A_t}\right)^2\frac{\left[1-(\frac{A_t}{A_2})^2\right]}{\left[1-(\frac{A_2}{A_1})^2\right]}(P_1-P_2)<0.8P_v \qquad (for\ critical\ flow\ with\ 20\%\ margin\ on\ P_v) \tag{27}$$

If control of the propellant's vapor pressure is possible, this equation can be used to choose the vapor pressure P_v that will choke an injector of a given geometry and for the desired operating pressures. Additionally, for a given geometry, upstream pressure P_1, and vapor pressure P_v, the downstream pressure P_2 corresponding to choking can be calculated directly. With the definition of a geometry based coefficient α as detailed below, the equations above can be manipulated into a simple and useful form for determining the downstream pressure P_2 corresponding to choking shown in Eq. (31) and Eq. (32):

$$\alpha=\left(\frac{C_{d,inj}}{C_{d,diff}}\right)^2\left(\frac{A_2}{A_t}\right)^2\frac{\left[1-(\frac{A_t}{A_2})^2\right]}{\left[1-(\frac{A_2}{A_1})^2\right]} \tag{28}$$

$$P_t=P_2-\alpha(P_1-P_2) \tag{29}$$

$$P_2 = \frac{P_t + \alpha P_1}{1 + \alpha} \tag{30}$$

$$P_2 = \frac{P_v + \alpha P_1}{1 + \alpha} \qquad (for\ critical\ flow\ with\ no\ margin) \tag{31}$$

$$P_2 = \frac{0.8P_v + \alpha P_1}{1 + \alpha} \qquad (for\ critical\ flow\ with\ 20\%\ margin\ on\ P_v) \tag{32}$$

If instead, the operating pressures upstream and downstream of the injector are known, as well as the vapor pressure P_v, an expression for the corresponding geometry required for choking can be obtained in a similar fashion, and is shown below in Eq. (34) and Eq. (35):

$$\frac{A_2}{A_t} = \sqrt{1 + \left(\frac{C_{d,diff}}{C_{d,inj}}\right)\left(\frac{P_2 - P_t}{P_1 - P_2}\right)\left[1 - \left(\frac{A_2}{A_1}\right)^2\right]} \tag{33}$$

$$\frac{A_2}{A_t} > \sqrt{1 + \left(\frac{C_{d,diff}}{C_{d,inj}}\right)\left(\frac{P_2 - P_v}{P_1 - P_2}\right)\left[1 - \left(\frac{A_2}{A_1}\right)^2\right]} \qquad (for\ critical\ flow\ with\ no\ margin) \tag{34}$$

$$\frac{A_2}{A_t} > \sqrt{1 + \left(\frac{C_{d,diff}}{C_{d,inj}}\right)\left(\frac{P_2 - 0.8P_v}{P_1 - P_2}\right)\left[1 - \left(\frac{A_2}{A_1}\right)^2\right]} \qquad (for\ critical\ flow\ with\ 20\%\ margin\ on\ P_v) \tag{35}$$

From examination of the equation above, it is clear that the important geometric parameter highlighted is the ratio of the injector exit area A_2 to the injector throat area A_t. It should be noted that the ratio of exit area A_2 to upstream area A_1 shows up on the right hand side of the equation. In a vast majority of injector designs, the value of (A_2/A_1) is close to zero, and due to the fact that it is squared in the equation, the term $[1 - (A_2/A_1)^2]$ is almost always negligible. This extends to all of the equations in this analysis, however, the term is kept in the analysis for completeness.

The discharge coefficients $C_{d,inj}$ and $C_{d,diff}$ do not depend strongly on the geometry of the diffuser and, again, are empirically determined as mentioned earlier. The injector discharge coefficient $C_{d,inj}$ usually ranges from values of approximately 0.61 to 0.9 and is highly dependent on the geometry of the injector inlet (rounded, chamfered, square edged, etc.), with a slight dependence on Reynolds number. The value of $C_{d,diff}$ is usually close to 1.0 and can be effected by the surface roughness of the diffuser surface. In cases where the flow separates within the diffuser, $C_{d,diff}$ can drop significantly away from unity, and the effectiveness of the device can be adversely affected. It is required that the diffuser section for these injectors is designed to avoid separation (i.e. minimize diffuser half angle).

C. Prototype Development and Cold Flow Testing

In order to provide a proof of concept of the novel injection scheme presented in this section, a demonstration of the critical flow behavior of a sample injector was performed in the cold flow test rig described in Ref. 5. For this proof of concept, the goal was to design an injector for use with cold nitrous oxide near -20 ^oC (253 K) at an upstream pressure of approximately 1000 psia (6.89 MPa), that would transition to the critical flow regime at a ΔP value in the range of 200-250 psi (1.38-1.72 MPa). Critical flow in this regime would occur with chamber pressures well above the vapor pressure of the nitrous oxide, and would sufficiently validate this technique.

1. Prototype Design

In order to achieve mass flow rate insensitivity at the operating conditions described above, a sample injector element was designed with a 0.059 inch (1.5 mm) throat diameter. An area ratio $A_2/A_t = 2$ was chosen in an attempt to achieve critical flow at the appropriate pressure drop, resulting in a required exit diameter of approximately 0.085 inches (2.15 mm). The inlet was slightly rounded, though unfortunately in the as built condition somewhat sharp edges did still exist (this will be evident from the measured discharge coefficient in the single phase region). The overall length of the injector element was kept the same as most of the designs described in Ref. 5, and therefore, the rate of expansion of the diffuser section was only required to be at a half-angle of 1^o. Due to this very narrow angle diffuser, there were no concerns about diffuser flow separation. A cross section of the prototype design is shown in Fig. 21.

This is clearly a moderate design for this new class of injector, so successful results in this series of tests would be highly encouraging in terms of the application of this concept to more aggressive operating constraints.

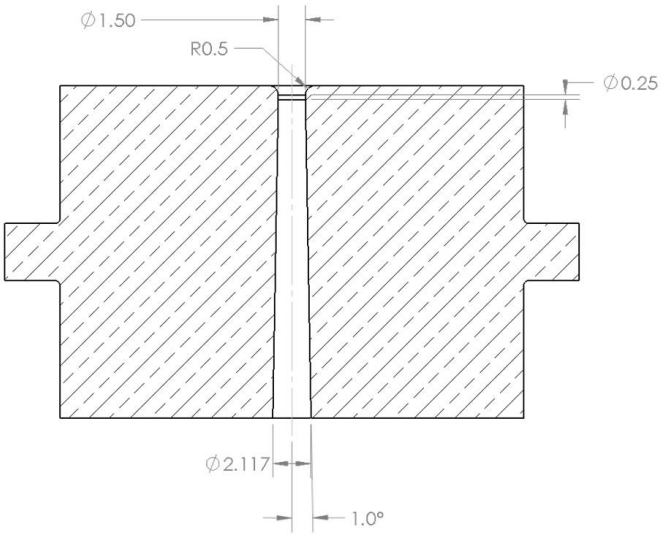

Figure 21. Cross-section of the novel injector prototype design (dimensions in *mm*).

2. *Cold Flow Testing*

Using the same cold flow test apparatus as described in Ref. 5, a series of cold flow tests were performed using the prototype injector with nitrous oxide at approximately -17 ^oC (256 K). The corresponding N_2O vapor pressure is approximately 286 psia (1.97 MPa). These tests were performed for range of supercharge values in order to sweep through many of the possible operating conditions that this sample injector could be practically applied. Fig. 22 shows the mass flow rate vs. chamber pressure P_2 for a variety of tests at varying levels of supercharge. The vertical red line on the plot indicates the value of the vapor pressure P_v for this set of tests. For the same set of tests Fig. 23 reports the effective discharge coefficient values vs. P_2. These tests clearly show that this prototype novel injector design was successful in achieving critical flow at chamber pressures well above vapor pressure. Examining the design point which determined the chosen geometry of the prototype, it can be seen that for the test at 972 psia (6.70 MPa) upstream pressure, the critical flow regime began when the chamber pressure reached approximately 720 psia (4.96 MPa), which corresponds to a pressure drop of approximately 238 psi (1.64 MPa). This is squarely in the range that was targeted by the design. It is also interesting to note the performance at low values of supercharge. Comparing these tests to those performed in Ref. 5 using standard straight hole injectors, it appears that the behavior enters the critical flow regime at higher values of P_2/P_v using the new injection scheme (see Fig. 12). This earlier transition is indeed expected based on the analysis presented above, but these results highlight that the use of this novel injection scheme is likely beneficial in efforts to suppress the feed system coupled instability even at off nominal operating conditions. It is safe to say that these cold flow tests were successful in achieving the proof of concept for the critical flow operation of the new injection scheme proposed in this section.

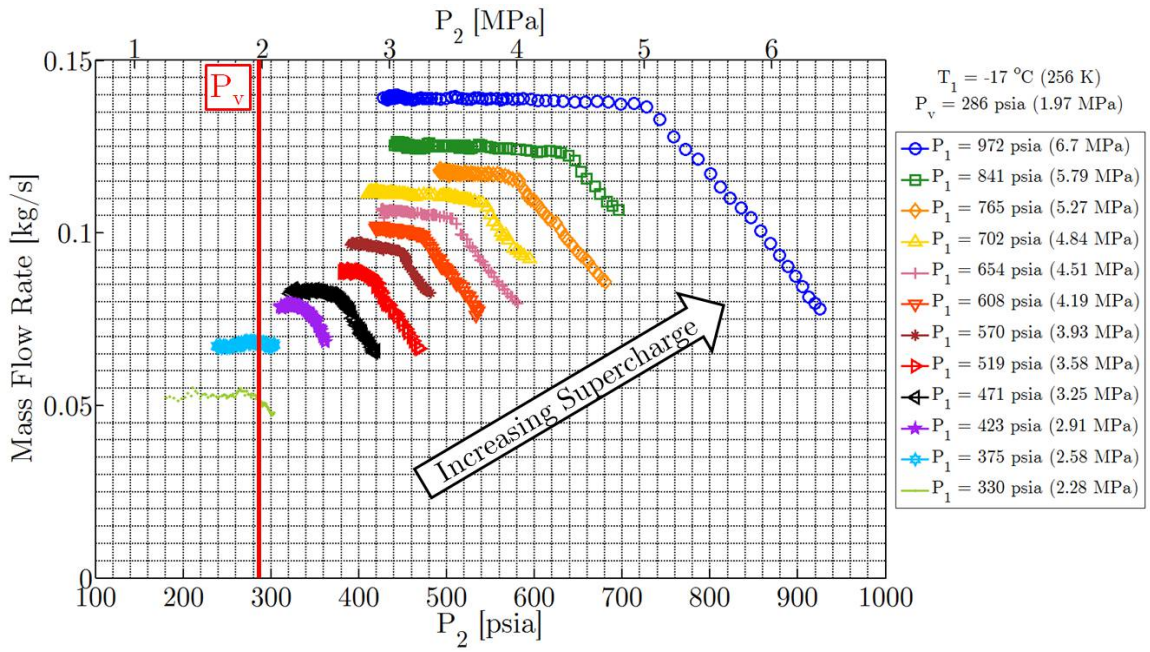

Figure 22. Measured $\dot{m}$ vs. P_2 during cold flow tests of the novel injector prototype using liquid N_2O at -17 ^oC (256 K) at various supercharge levels.

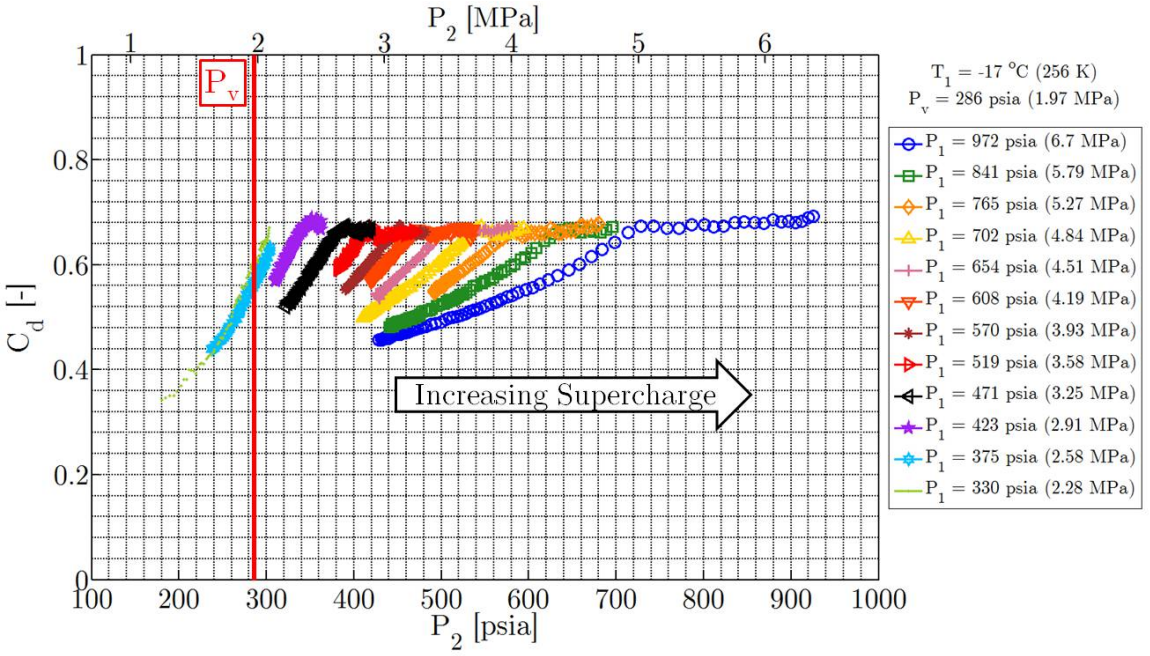

Figure 23. Measured C_d vs. P_2 during cold flow tests of the novel injector prototype using liquid N_2O at -17 ^oC (256 K) at various supercharge levels.

V. Summary and Conclusions

Low frequency combustion instabilities have proven to be a major obstacle for hybrid rocket development programs over the past few decades. The feed system coupled combustion instability has been particularly problematic for hybrid rocket development programs utilizing nitrous oxide as the oxidizer. While cavitating venturis can be used as isolation elements in order to eliminate the feed system coupled instability from hybrid rockets which use LOX, the risk of a decomposition reaction explosion prohibits this solution for nitrous oxide systems. However, based upon

the small scale injector cold flow results from Ref. 5, it was determined that a critical flow injector could provide the necessary isolation to suppress the feed system coupled instability. This theory was tested in the full scale Peregrine Sounding Rocket heavyweight combustion facility with tremendous success, leading to highly stable combustion. The results from Tests E3-4 and E4-1 signal a major step forward in the understanding and suppression of combustion instabilities in hybrid rocket motors, not only for the Peregrine Sounding Rocket program, but for the industry as a whole.

The critical injector flow criteria for suppressing the feed system coupled instability developed in Section III can be extremely useful, but typically comes at the cost of overall rocket system performance and requires restrictions on the possible operating conditions of the motor. However, the novel injection scheme presented in this section addresses both of these shortcomings. Based on the results from a series of cold flow tests of this novel injection scheme, the author is highly encouraged that this style of injector could be used in an actual hybrid rocket motor resulting in significant improvements to both stability and performance. No hybrid rocket hot fire tests using this style of injector have been performed in the Peregrine heavyweight combustion facility to date, but there are plans to do so in the future. It is expected that this technology will be adopted in the design of many current and future nitrous oxide based hybrid rockets in order to promote stable combustion. Additionally, while this new class of injector was certainly conceived of with nitrous oxide hybrid rockets in mind, it can be applied to any liquid rocket feed system, even those using traditional low vapor pressure propellants.

VI. Future Work

Continued cold flow testing of the novel injection scheme presented in this work should be aimed at characterizing the design limitations with relation to critical flow. It would be useful to develop a set of guidelines pertaining to the allowable diffuser divergence angles and design criteria to ensure the flow remains attached within the diffuser section. Also, cold flow tests with some traditional low vapor pressure oxidizers such as LOX (or liquid nitrogen as an analog) should be performed to demonstrate the usefulness of this technology for a broad range of rocket applications.

Additionally, further cold flow testing should be used to study the effects of dissolved gas and its desorption on the inception of cavitation and critical flow within the injector. Not only should these types of studies be performed for the typically inert pressurant gases that are dissolved in nitrous oxide such as helium, but also reactive pressurants such as oxygen. This is of interest based on the possible use of a new and exciting class of oxidizer called Nytrox [23], as well as for the design of hybrid rockets that use the pressurant as a propellant, the advantages of which are described by Chandler et al. in Ref. 24.

Finally, next steps in the full scale Peregrine Sounding Rocket development program should include hot fire testing using the cavitating venturi style injector. While cold flow studies have proven that an appropriately designed cavitating venturi injector should provide critical flow under conditions which would improve the overall performance of the Peregrine hybrid rocket, the ability to suppress the feed system coupled instability under these conditions has not been demonstrated as of yet.

Acknowledgments

This work was supported in part by the National Defense Science and Engineering Graduate Fellowship Program (NDSEG) and the Aeronautics and Astronautics Department at Stanford University. Additionally, some of the work on the Peregrine Sounding Rocket was supported by the National Aeronautics and Space Administration under Prime Contract Number NAS2-03144 awarded to the University of California, Santa Cruz, University Affiliated Research Center (UARC) as well as the NASA Ames Research Center Fluid Mechanics Lab.

References

[1]Dyer, J., Doran, E., Dunn, Z., Lohner, K., Bayart, C., Sadhwani, A., Cantwell, B., and Karabeyoglu, A., "Design and Development of a 100 km Nitrous Oxide / Paraffin Hybrid Rocket Vehicle," *43rd AIAA/ASME/SAE/ASEE Joint Propulsion Conference and Exhibit*, Cincinnati, OH, July 2007.

[2]Thicksten, Z., Macklin, F., and Campbell, J., "Handling Considerations of Nitrous Oxide in Hybrid Rocket Motor Testing," *44th AIAA/ASME/SAE/ASEE Joint Propulsion Conference and Exhibit*, Hartford, CT, July 2008.

[3]Lemmon, E. W., Huber, M., and McLindon, M., "NIST Standard Reference Database 23: Reference Fluid Thermodynamic and Transport Properties-REFPROP, Version 930," 2010.

[4]Lemmon, E. W. and Span, R., "Short Fundamental Equations of State for 20 Industrial Fluids," *Journal of Chemical Engineering Data*, Vol. 51, 2006, pp. 785–850.

[5]Waxman, B. S., Zimmerman, J. E., Cantwell, B. J., and Zilliac, G. G., "Mass Flow Rate and Isolation Characteristics of Injectors for Use with Self-Pressurizing Oxidizers in Hybrid Rockets," *49th AIAA/ASME/SAE/ASEE Joint Propulsion Conference and Exhibit*, San Jose, CA, Aug. 2013, pp. 1–32.

[6]Waxman, B. S., *An Investigation of Injectors for Use with High Vapor Pressure Propellants with Applications to Hybrid Rockets*, Ph.D. thesis, Stanford University, 2014.

[7]Zilliac, G., Waxman, B. S., Doran, E., Dyer, J., Karabeyoglu, M. A., and Cantwell, B., "Peregrine Hybrid Rocket Motor Ground Test Results," *48th AIAA/ASME/SAE/ASEE Joint Propulsion Conference and Exhibit*, Atlanta, GA, Aug. 2012.

[8]Karabeyoglu, M. A., Altman, D., and Cantwell, B. J., "Combustion of Liquefying Hybrid Propellants : Part 1 , General Theory," *Journal of Propulsion and Power*, Vol. 18, No. 3, 2002, pp. 610–620.

[9]Chadler, A. A., *An Investigation of Liquefying Hybrid Rocket Fuels with Applications to Solar System Exploration*, Ph.D. thesis, Stanford University, 2012.

[10]Cantwell, B., Karabeyoglu, A., and Altman, D., "Recent Advances in Hybrid Propulsion," *International Journal of Energetic Materials and Chemical Propulsion*, Vol. 9, No. 4, 2010, pp. 305–326.

[11]Zilliac, G., Waxman, B. S., Evans, B., Karabeyoglu, M. A., and Cantwell, B., "Peregrine Hybrid Rocket Motor Development," *AIAA Propulsion and Energy Conference*, Cleveland, OH, July 2014.

[12]Walker, J. S., *Fast Fourier Transforms*, Vol. 24, CRC press, 1996.

[13]Sutton, G. and Biblarz, O., *Rocket Propulsion Elements*, Wiley and Sons, New York, 7th ed., 2001.

[14]Cohen, J. M., Proscia, W., and Delaat, J., "Longitudinal-Mode Combustion Instabilities: Modeling and Experiments," Tech. Rep. May, NASA, 2000.

[15]Blomshield, F. S., "Lessons Learned in Solid Rocket Combustion Instability," *AIAA Missile Sciences Conference*, Monterey, CA, Nov. 2006.

[16]Karabeyoglu, M. A., Zilwa, S. D., Cantwell, B., and Zilliac, G., "Transient Modeling of Hybrid Rocket Low Frequency Instabilities," *39th AIAA/ASME/SAE/ASEE Joint Propulsion Conference and Exhibit*, July 2003.

[17]Yang, V. and Anderson, W., "Liquid Rocket Engine Combustion Instability," *Progress in Astronautics and Aeronautics*, Vol. 169, 1995.

[18]Karabeyoglu, A., Stevens, J., and Cantwell, B., "Investigation of Feed System Coupled Low Frequency Combustion Instabilities in Hybrid Rockets," *43rd AIAA/ASME/SAE/ASEE Joint Propulsion Conference and Exhibit*, No. July, Cincinnati, OH, July 2007.

[19]Carpenter, R. L., Boardman, T. A., and Claflin, S. E., "Hybrid Propulsion for Launch Vehicle Boosters : A Program Status Update," *31 st AIAA / ASME / SAE / ASEE Joint Propulsion Conference and Exhibit*, San Diego, CA, July 1995.

[20]Rocker, M., "Modeling of Nonacoustic Combustion of Hybrid Instability in Simulations Motor Tests," Tech. rep., NASA, 2000.

[21]Randall, L., "Rocket Applications of the Cavitating Venturi," *Journal of the American Rocket Society*, Vol. 22, No. 1, 1952, pp. 28–38.

[22]Karabeyoglu, A., Dyer, J., Stevens, J., and Cantwell, B., "Modeling of N2O Decomposition Events," *44th AIAA/ASME/SAE/ASEE Joint Propulsion Conference and Exhibit*, Hartford, CT, July 2008.

[23]Karabeyoglu, M. A., "Nitrous Oxide and Oxygen Mixtures (Nytrox) as Oxidizers for Rocket Propulsion Applications," *Journal of Propulsion and Power*, Vol. 30, No. 3, May 2014, pp. 696–706.

[24]Chandler, A. A., Cantwell, B. J., Hubbard, G. S., and Karabeyoglu, A., "Feasibility of a single port Hybrid Propulsion system for a Mars Ascent Vehicle," *Acta Astronautica*, Vol. 69, No. 11-12, Dec. 2011, pp. 1066–1072.